Ames

NASA Technical Memorandum 88349

245

Calculated Performance, Stability, and Maneuverability of High-Speed Tilting-Prop-Rotor Aircraft

Wayne Johnson, Benton H. Lau, and Jeffrey V. Bowles

September 1986

National Aeronautics and
Space Administration

NASA Technical Memorandum 88349

Calculated Performance, Stability, and Maneuverability of High-Speed Tilting-Prop-Rotor Aircraft

Wayne Johnson,
Benton H. Lau,
Jeffrey V. Bowles, Ames Research Center, Moffett Field, California

September 1986

National Aeronautics and
Space Administration

Ames Research Center
Moffett Field, California 94035

CALCULATED PERFORMANCE, STABILITY, AND MANEUVERABILITY OF HIGH-SPEED TILTING-PROP-ROTOR AIRCRAFT

Wayne Johnson, Benton H. Lau, and Jeffrey V. Bowles
NASA Ames Research Center, Moffett Field, CA 94035 USA

1. ABSTRACT

The feasibility of operating tilting-prop-rotor aircraft at high speeds is examined by calculating the performance, stability, and maneuverability of representative configurations. The rotor performance is examined in high-speed cruise and in hover. The whirl-flutter stability of the coupled-wing and rotor motion is calculated in the cruise mode. Maneuverability is examined in terms of the rotor-thrust limit during turns in helicopter configuration. The paper discusses rotor airfoils, rotor-hub configuration, wing airfoil, and airframe structural weights represent demonstrated advanced technology. Key rotor and airframe parameters are optimized for high-speed performance and stability. The basic aircraft-design parameters are optimized for minimum gross weight. To provide a focus for the calculations, two high-speed tilt-rotor aircraft are considered: a 46-passenger, civil transport and an air-combat/escort fighter, both with design speeds of about 400 knots. It is concluded that such high-speed tilt-rotor aircraft are quite practical.

2. NOMENCLATURE

A	prop-rotor disk area
C_{m_x}	blade-beam, bending-moment coefficient, $NM_x/\rho A(\Omega R)^2 R$
C_p	prop-rotor power coefficient, $P/\rho A(\Omega R)^3$
C_T	prop-rotor thrust coefficient, $T/\rho A(\Omega R)^2$
FLIR	Forward-Looking Infrared Radar
IRP	intermediate-rated power
JVX	Joint Services Advanced Vertical-Lift Aircraft
LHX SCAT	Light Helicopter Family: Scout/Attack
M	figure of merit, $0.707\, C_T^{3/2}/C_P$
M_{at}	for helicopter operation, advancing-tip Mach number; for propeller operation, helical-tip Mach number
M_{tip}	tip Mach number, ΩR divided by speed of sound

M_x	blade-beam bending moment
N	number of blades
P	prop-rotor power
R	prop-rotor radius
r	blade-radial station, measured from center of rotation
T	prop-rotor thrust
TADS	Target-Acquisition and Designation System
V	aircraft speed
v	prop-rotor induced velocity
W	aircraft gross weight
α_P	pylon angle; zero for propeller operation, 90° for helicopter operation
δ_3	pitch-flap coupling
ρ	air density
σ	prop-rotor solidity, blade area divided by disk area
Ω	prop-rotor rotational speed

3. INTRODUCTION

The tilting-prop-rotor aircraft concept has been demonstrated by the NASA/Army XV-15 Tilt Rotor Research Aircraft (Fig. 1). The XV-15 has been flown to 260 knots at sea level, and to 300 knots at 16,000-ft altitude. The XV-15 was developed to demonstrate the solution of the key technical problems of the tilt-rotor configuration, particularly the issue of high-speed aeroelastic stability. The proof-of-concept flight tests of the XV-15 were completed in 1981, and the aircraft has been used since then in numerous operational suitability demonstrations and technical investigations.

The tilt-rotor concept is going into production with the V-22 Osprey (Fig. 2), being developed by the U.S. Navy. The V-22 will operate to 280 knots at sea level, and to 335 knots at 18,000 ft. This maximum speed capability is typical of turboprop transports in the 40,000-lb gross weight class, and is appropriate for a military-transport aircraft with an operational radius of 230 mi (in the marine assault role).

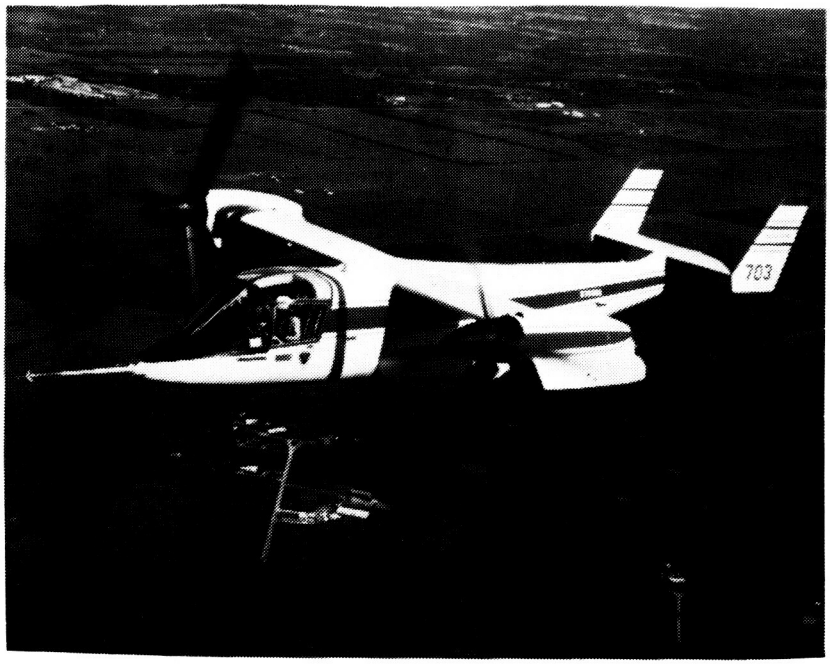

Fig. 1. NASA/Army XV-15 Tilt Rotor Research Aircraft.

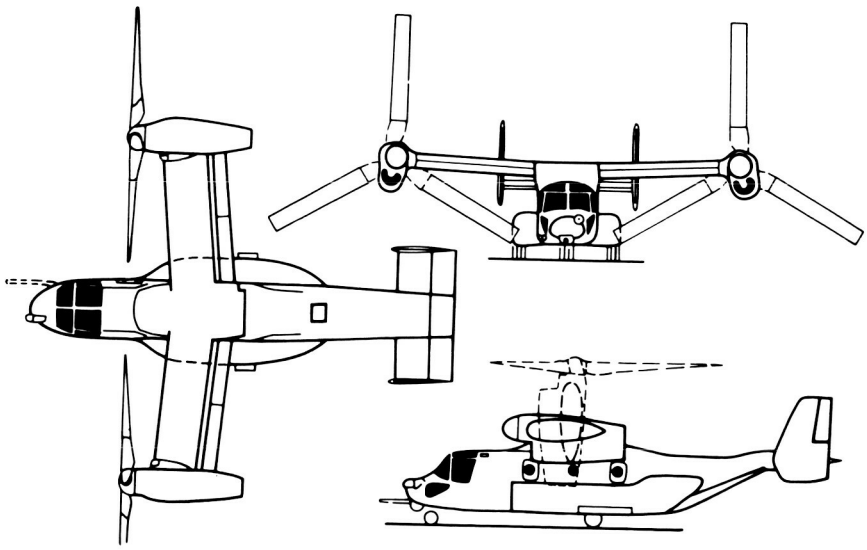

Fig. 2. V-22 Osprey tilting-prop-rotor aircraft.

An important question that remains is exactly where the tilt-rotor concept fits in the spectrum of aircraft configurations--especially regarding the maximum speeds of aircraft with vertical takeoff and landing capability. This paper examines the feasibility of operating tilting-prop-rotor aircraft at high speeds. A comprehensive rotorcraft analysis was used to calculate the aeromechanical behavior (performance, stability, and maneuverability) of tilt-rotor aircraft, and to optimize the rotor and wing characteristics for high-speed operation. A preliminary design analysis was used to size representative tilt-rotor aircraft for specific high-speed missions. To provide a focus for the calculations, two high-speed tilt-rotor aircraft are considered: a

46-passenger civil transport and an air-combat/escort fighter, both with design speeds of about 400 knots.

The objective of this paper is to explore the technical obstacles to achieving a major increase in the maximum speed capability of tilt-rotor aircraft. The target of a maximum speed of 400 knots constitutes a significant increase in capability, and might indeed be faster than required by many subsonic missions. If it can be established that there are no technical barriers to achieving that speed (subject perhaps to some research and development requirements), then it will be possible to begin the task of balancing the value and cost of such speed capability to optimize the aircraft for specific mission requirements.

4. APPROACH

The characteristics of high-speed tilting-prop-rotor aircraft are examined using a combination of preliminary design and aeromechanics analyses. To begin, calculations for the XV-15 are used to discuss the behavior of tilt-rotor aeromechanics, and to illustrate the correlation of the analysis. Then the influence of advanced technology is considered, including advanced rotor airfoils and hub, and an advanced-wing airfoil. Next, the rotor aerodynamics are optimized for good performance at high speed, and the aircraft dynamics are optimized for adequate stability margin. Finally, two specific high-speed designs are examined: a civil transport and an air-combat/escort fighter. In particular, the weight and power of these designs will illustrate the feasibility of such high speed capability in tilting-prop-rotor aircraft.

4.1. Performance, Stability, and Maneuverability Characteristics

The performance characteristics examined are the propulsive efficiency in high-speed cruise, and the hover figure of merit. The efficiency parameter used for axial flow is the ratio of the prop-rotor ideal power to the actual power: $T(V+v)/P$, where v is the induced velocity calculated by momentum theory. This parameter is the rotor figure of merit in hover ($V = 0$), and is nearly equal to the propulsive efficiency TV/P in cruise (where v/V is small). The efficiency was calculated for an isolated rotor as a function of thrust for a given flight speed and tip speed. For a high-speed tilt-rotor, cruise rather than hover determines the installed power. Hence for the present purposes, hover performance is examined only to ensure the absence of major adverse effects of the optimization for high speed.

The principal dynamics problem of tilting-prop-rotor aircraft in cruise flight is whirl flutter. Whirl flutter is the coupled motion of the prop-rotor and the aircraft (typically the wing elastic modes) that becomes unstable at high forward speed because of the rotor aerodynamic forces. The rigid body and elastic motion of the blades makes tilt-rotor whirl flutter a different, and more complicated, phenomenon than the whirl flutter of a propeller-driven airplane. The stability is

defined by the damping ratio of the wing modes as a function of flight speed, calculated in airplane configuration (0° pylon angle). Six wing modes are considered: symmetric and antisymmetric wing beam, chord, and torsion motion. The aircraft is trimmed to level flight or in a descent at maximum power (the stability boundary will be well beyond the level flight capability of the aircraft). For a tilt-rotor at sea level, the maximum power limit is determined by the transmission torque capability, not by the power available from the engine. It is necessary to select the wing stiffness to ensure that the stability boundary is sufficiently beyond the operating speed (for example, 1.25 times maximum speed).

The aircraft maneuverability is here characterized by the rotor thrust limit in turns at moderate speed, with the aircraft in helicopter configuration. In turns the blade loads and power would increase steeply at rotor stall if the aircraft were to maintain level flight. However, with a fixed amount of power available, the tilt-rotor begins to descend at a moderate rate when rotor lift limit is reached. Hence, although the limit is well defined, it is benign operationally. The lift limit of the rotor optimized for high-speed performance then determines the wing loading required to achieve the desired maneuver capability. For this paper, the rotor lift limit was calculated at only one operating condition, representative of a low-speed maneuver requirement: 90 knots, with a 75° pylon angle (tilted 15° from helicopter configuration). The aircraft was trimmed to a specified turn rate in level flight or at maximum power (again, as determined by the transmission torque limit).

4.2. Design Mission Requirements

The civil transport was sized to carry 46 passengers (9000-lb payload) on a 600-n. m. mission, with a cruising speed of 375 knots at normal-rated power at an altitude of 20,000 ft. The mission included vertical flight at the takeoff and landing points, and a reserve leg consisting of a 100-n. m. alternate plus 45 min hold. This mission is representative of a commuter or regional carrier flight profile, but at a higher speed than typically flown by current turboprop commuter aircraft.

The air combat vehicle was sized to perform a land-assault-troop escort mission. The mission radius was 200 n. m., with a combination of low-speed loiter and a high-speed IRP dash at the midpoint. Mission cruise legs were flown at a 3000-ft altitude and 91.5°F ambient temperature at a cruise speed of 265 knots (the best specific range speed of a troop transport, such as the V-22). The engine and rotor were designed for a 400-knot capability, but aircraft speed at sea level was transmission limited to 365 knots. This limit results in a vehicle weight savings. The 400-knot capability is achievable at higher altitude (15,000 to 20,000 ft). A 20-min loiter requirement for fuel reserves at the end of the mission was also imposed. The vehicle was sized for a single pilot and 2200 lb of mission equipment, including 1200 lb of ordnance. This mission package weight is representative of the

LHX-SCAT-mission equipment requirement. No specific aircraft-load factor capability was considered, but the maneuver capability was a factor in selecting the blade loading and wing loading in the design process.

5. ANALYSES

5.1. Preliminary Design

The preliminary design and performance code used in this study was developed jointly by the U.S. Army Aviation Systems Command and the NASA Advanced Plans and Programs Office at Ames Research Center. This synthesis code estimates the performance of tilt-rotor aircraft based on the input mission requirements and constraints. Vehicle weight, power, and geometric characteristics that meet the input design requirements and the technology-level assumptions are then computed. The code has been used by both the Army and NASA as part of the JVX Joint Technology Assessment study, the preliminary design studies in support of LHX, and several in-house systems-study activities.

The code models various technology disciplinary areas, including weights, airframe and rotor aerodynamics, propulsion system, and vehicle-performance estimation. The analytical models and the associated input data are generally calibrated using either experimental test results (such as rotor performance) or predicted results from detailed analysis codes. The synthesis code iterates on the gross weight to size the vehicle until the mission and performance constraints and requirements are satisfied.

The weight estimates for the various aircraft components are calculated by correlating statistical trends based on existing aircraft designs (such as the XV-15) and by dimensional analysis of generic component designs. The weight-trend equations are generated by a multiple-regression-analysis method, correlated with either physical or geometric characteristics or with requirements that most significantly influence the component-group weight. Where applicable, advanced-technology factors are applied to the component weight to reflect the expected weight reduction resulting from the application of advanced materials.

For tilt-rotor aircraft with rotor-system designs similar to that of the V-22 or XV-15, the wing design is dictated by the wing/pylon aeroelastic-stability requirements, and not by usual fixed-wing, bending moment criteria. The wing is sized using dynamic similarity rules (dimensionless frequency ratios) to meet vertical-, chord-, and torsion-stiffness requirements determined by aeroelastic stability margins. In addition, a 2-g jump takeoff requirement is checked to see whether additional spar cap material is needed.

Airframe aerodynamics are estimated using empirical methods calibrated with wind tunnel and flight-test data. Using the XV-15 as a baseline configuration, a component-profile drag buildup is computed,

with corrections for relative changes in Reynolds number, wetted area, and interference drag. Incremental drag area is added to represent the drag of externally mounted mission equipment (such as FLIR system or a gun turret). Wing-induced drag is computed as a function of wing lift coefficient and wing-aspect ratio. The tip-mounted nacelles are assumed to provide an end-plating effect, giving an Oswald efficiency factor close to unity. Hover download is computed as a function of rotor and wing geometry, with provision for download alleviation devices.

The rotor aerodynamic performance is estimated using simplified analytical models calibrated by both test data and detailed performance analyses. The rotor-induced power is calculated using momentum theory with nonuniform inflow and tip-loss factors applied. The rotor profile power is computed as a function of thrust weighted C_T/σ, with a correction factor applied for advance ratio effects. Again, the correction factors for both induced and profile power are determined by test or detailed analysis results. To examine high-speed tilt-rotor performance, the design code had to be modified to include both wing- and rotor-compressibility effects.

Propulsion-system performance is computed using curve-fitted models of engine power, fuel flow, airflow, and tailpipe thrust as a function of power setting, engine revolutions per minute, flight speed, altitude, and ambient temperature. For tilt-rotor concepts, the rotor-tip speed is reduced in the airplane's cruise mode, so modeling the engine performance for off-design engine speed is necessary. With the required rotor power computed, transmission power loss (a function of torque), accessory power extraction, and IR suppression losses are then added to determine required engine power. Momentum drag losses caused by the suppression of the cooling flow (if required) are included as part of required prop-rotor thrust. The user can evaluate fixed-sized engine performance, or have the design code size the engine to meet mission requirements. The latter approach was used for the present investigation.

The synthesis design code predicts the hover, conversion, and airplane-mode performance for steady-state, level-flight conditions. The mission performance is computed with a series of hover and forward-flight segments flown for an input time or distance, with mission fuel computed as a sum of the fuel burned for each segment. Off-design mission performance can also be determined.

To begin the study, the two high-speed tilt-rotor designs were sized for their respective missions using V-22 aerodynamic and structural technology levels to model rotor, wing, and structure. For an initial estimate of expected advanced-technology rotor design, the prop-rotor drag-divergence Mach number was increased by 8%. The computed aircraft design characteristics were then used in the aeromechanics analysis as a starting point. These baseline designs were also used to perform sensitivity calculations to determine the driving technology requirements for high speed tilt-rotor applications. The engine

technology selected for the study was representative of state-of-the-art high-performance turboshaft designs.

5.2. Aeromechanics Calculations

The aeromechanics calculations were performed using the Comprehensive Analytical Model of Rotorcraft Aerodynamics and Dynamics (CAMRAD). This code, designed to handle tilting-prop-rotor aircraft as well as helicopter configurations, provides performance, blade loads, and aeroelastic stability results from a single, consistent formulation. The analysis is described fully in Refs. 1-3. The levels of modeling complexity sufficient for accurate performance, loads, and stability calculations were established in earlier work [4,5].

The analysis trims the aircraft to a specified flight condition by adjusting the pilot's controls and aircraft attitude. For stability calculations, the aircraft was trimmed in level flight at a given speed, or in a climb or descent at a given speed and power. For maneuverability calculations, the aircraft was trimmed in level flight or to maximum power at a given speed and turn rate. For performance calculations, an isolated rotor in hover or cruise was trimmed to a specified thrust.

The degrees of freedom used in the calculations are shown in Table 1. The trim solution involves the periodic rotor motion, while the flutter solution concerns the perturbed motion of the rotor and airframe. The flutter analysis is performed separately for symmetric and antisymmetric aircraft motions (each with 18 degrees of freedom for a three-bladed rotor and 21 degrees of freedom for a four-bladed rotor). Ten harmonics were used in the periodic-motion solution when the maneuverability was calculated (for accurate blade loads in helicopter forward flight), two harmonics were used when the aircraft was trimmed for stability calculations (in airplane mode cruise flight), and no harmonics were used (only static deflection) for performance calculations in hover and cruise flight (axial flow).

Static, two-dimensional, airfoil characteristics were used in the rotor aerodynamics analysis, with corrections for yawed flow effects and a tip-loss factor. The key airfoil characteristics influencing tiltrotor behavior are the lift-curve slope (high-speed stability), the drag-divergence Mach number (cruise performance), the maximum lift coefficient (hover performance and maneuverability), and the minimum drag coefficient (performance). An azimuthal increment of 15° was used for the periodic motion solution. Fifteen radial stations, concentrated toward the blade tip, were used for the aerodynamic analysis of the rotor.

The rotor's wake-induced velocity used in the calculations was constant over the rotor disk for hover and cruise (axial-flow conditions), and varied linearly over the rotor disk for helicopter forward flight. The mean induced velocity was obtained from momentum theory, with the ideal value multiplied by an appropriate factor to account for

Table 1. Degrees of freedom used in aeromechanics calculations

	Analysis task			
	Performance	Loads	Stability	
			Trim	Flutter
Rotor				
Gimbal pitch and roll	Yes	Yes	Yes	Yes
Rotational speed	None	None	None	Yes
Dynamic inflow	None	None	None	Quasi-static
Each blade				
Coupled flap/lag bending	2 modes	3 modes	2 modes	2 modes
Rigid pitch motion	Yes	Yes	None	Yes
Elastic torsion	Yes	None	None	None
Airframe				
Rigid body	None	None	None	3 modes
Elastic	None	None	None	3 modes
Governor	None	None	None	Quasi-static
Total number	5	5	3	18-21

nonideal induced power losses. The induced velocity is small compared with the flight velocity in propeller mode operation. Therefore, the approximation of uniform inflow is not significant for the crucial flight conditions of this paper.

Nonuniform inflow has a significant influence on the blade airload distribution in hover, and must be considered for a realistic calculation and optimization of hover performance. Since in this paper hover is not a crucial design condition, for simplicity a uniform inflow model was used. Nonuniform inflow influences the calculation of rotor loads and power in helicopter forward flight. To determine the maximum-lift capability, which is characterized by a massive stall of the rotor, it should be sufficient to use the uniform inflow model.

6. TILT-ROTOR AEROMECHANICS BEHAVIOR

The aeromechanics behavior of tilt-rotor aircraft is examined in terms of calculations for the XV-15 Tilt Rotor Research Aircraft. Illustrative correlations of the comprehensive analysis with wind tunnel and flight test data are presented. The XV-15 technology level is therefore the starting point for the development of high-speed designs.

6.1. Performance

Good prop-rotor efficiency at high speed depends on low rotor-blade drag at high Mach numbers. The drag-divergence Mach number should be high; then the prop-rotor can be operated at high tip speed, minimizing the blade area required. The compromise between helicopter and airplane configurations means that the rotor operates at a relatively low blade loading as a propeller. While the blade area is therefore higher than needed for optimum cruise, the C_T/σ is high enough so that there is little penalty in propulsive efficiency. Figure 3 compares the calculated propulsive efficiency for the XV-15 rotor with full-scale wind tunnel measurements [6]. A typical operating point for the XV-15 is $C_T/\sigma = 0.05$. In Fig. 3 the maximum Mach number is well below drag divergence, so both calculations and measurements show little influence of $V/\Omega R$ and Mach number. Additional correlation of the analysis with wind tunnel and flight measurements of the XV-15 cruise performance are given in Ref. 5.

Good prop-rotor efficiency in hover depends primarily on a high maximum-lift coefficient. The high disk loading of tilt-rotor designs produces a high figure of merit (i.e., the profile power is a small fraction of the total hover power); hence, the efficiency is less sensitive to the airfoil drag coefficient than for a helicopter rotor. It is desirable to operate the rotor at a relatively high blade loading in hover to minimize the blade area (which will still be too large in cruise). Operating at a high C_T/σ is possible because the edgewise flight limit on C_T/σ is less severe for a tilt-rotor because of the

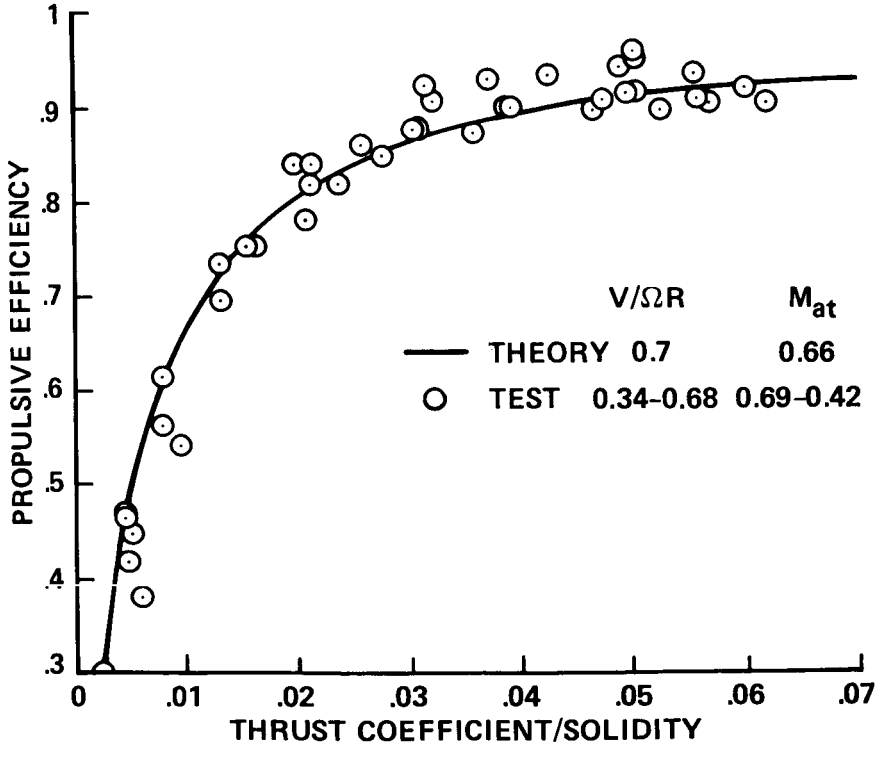

Fig. 3 XV-15 rotor propulsive efficiency; full-scale wind tunnel test results.

wing, and the lower maximum speed in helicopter configuration. Good blade stall characteristics increase the range of blade loading for which the figure of merit remains high. Wing download is included in the preliminary design analysis; it is a crucial factor for a hover-designed tilt-rotor, but it is not a design driver for a high-speed aircraft. Figure 4 compares the calculated hover figure of merit for the XV-15 rotor with full scale isolated-rotor measurements [7]. A typical operating point for the XV-15 is $C_T/\sigma = 0.13$. For hover calculations in this paper, a uniform induced velocity was used, equal to 1.085 times the ideal momentum theory value (the factor selected to achieve good correlation with the test data).

6.2. Maneuverability

From previous experience, the critical loads on the XV-15 rotor have been identified as follows: a) the oscillatory beamwise bending moment at 35% radial station (measured relative to the blade principal axes); b) the oscillatory spindle chord-bending moment (measured just inboard of the blade-pitch bearing and outboard of the spindle/yoke junction); and c) the oscillatory pitch-link load. The oscillatory load is one-half the difference between the maximum and minimum load values occurring in a rotor revolution. Figure 5 compares the calculated oscillatory beamwise bending moment on the XV-15 blade with flight-test measurements. Additional correlation of the analysis with wind tunnel and flight measurements of the XV-15 blade loads are given in Ref. 5, for helicopter, tilt-rotor, and cruise configurations.

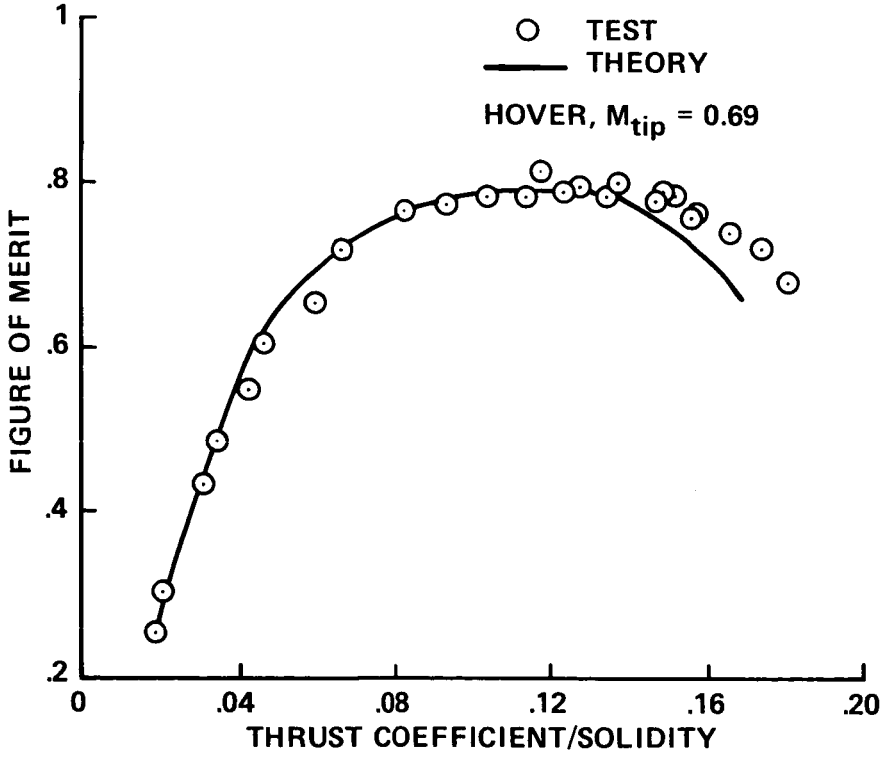

Fig. 4. XV-15 rotor hover figure of merit; full-scale isolated-rotor test results.

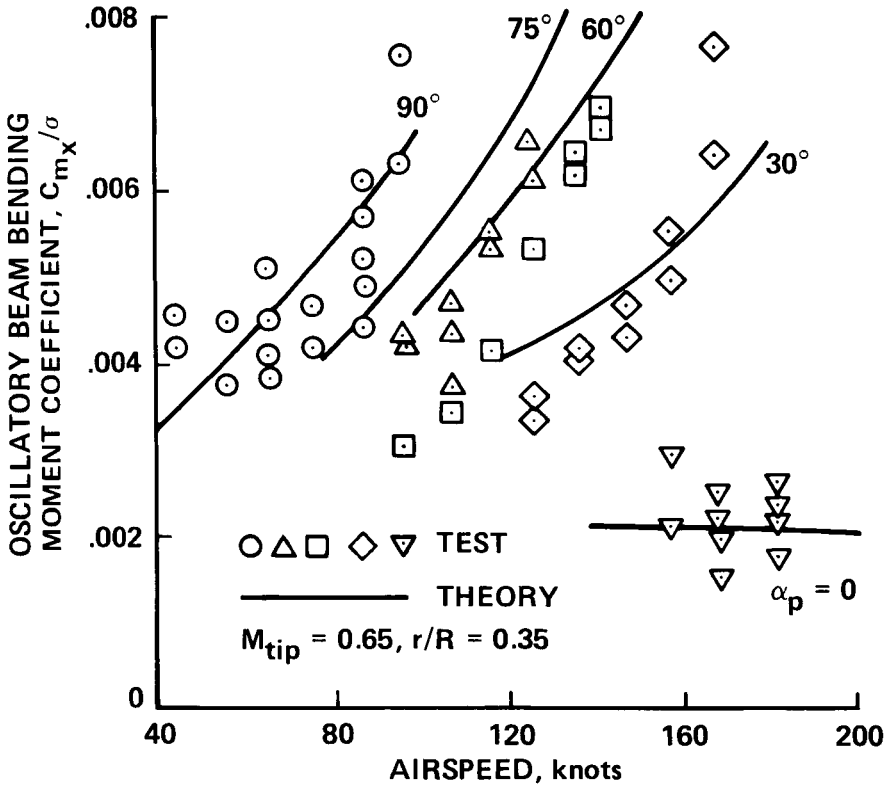

Fig. 5. XV-15 beamwise bending moment for rotor-blade oscillation; flight-test results.

During maneuvers the rotor loads are important because they limit the maximum rotor lift capability in helicopter or tilt-rotor configuration. Although the loads before the rotor stalls would be of concern in the final structural design of the aircraft, the present analyses are not being carried that far. It is found that the lift limit is defined by an abrupt rise in all the rotor loads, as well as the rotor power, so the level of loads below stall does not influence the lift limit significantly.

The XV-15 has achieved 1.75- to 2.0-g turns at around 100 knots in tilt-rotor configuration (pylon angle between 0 and 90°). It has been the experience of the Tilt Rotor Research Aircraft project at Ames Research Center that the effects of blade stall are not observed in the rotor loads during such maneuvers. The behavior is interpreted as that rotor speed governor reducing collective pitch in response to a revolution-per-minute droop if the rotor approaches stall. Hence, stall of the prop rotor is not a rotor-load problem, it only manifests itself as the inability to maintain level flight.

Figures 6 and 7 show the calculated blade oscillatory beamwise bending moment and rotor power as a function of rotor thrust for the XV-15 in a steady turn at 90 knots and a pylon angle of 75°. The thrust variation corresponds to increasing turn rate, with 1.0-g flight at the lowest thrust point shown in both figures. The calculated behavior shown is confirmed by the flight-test experience discussed in the

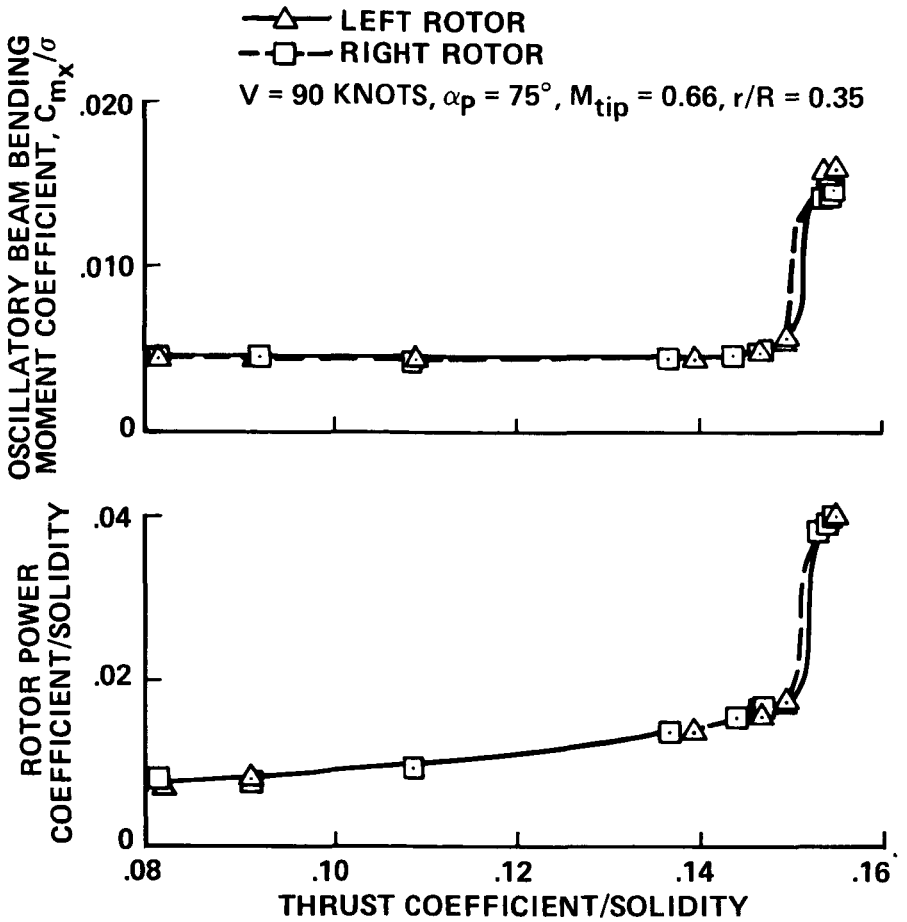

Fig. 6. Calculated XV-15 behavior in steady turns (level flight).

preceding paragraph. The wing carries significant lift at 90 knots, so in level flight (Fig. 6) the rotor $C_T/\sigma = 0.081$ at 1.0 g. There is little increase in blade stresses as the load factor increases, up to about $C_T/\sigma = 0.15$ (at a turn rate of 16.4°/sec here). Then, as a result of rotor stall, there is an abrupt rise in loads and power. The steepness of the boundary is increased by the aircraft trim changes when the rotor stalls. The rotor tip-path plane flaps aft relative to the shaft. The aircraft pitch angle then decreases to maintain trim, thereby decreasing the wing angle of attack and wing lift. Thus, more lift is demanded from the rotor, which drives the rotor even deeper into stall. Consequently, the calculation points just before and after the loads rise are only 0.1°/sec apart. At the point just before the rise, the rotor is operating with only a moderate amount of stall, typical of helicopter forward flight. At the next point, most of the rotor disk is stalled.

In level flight, the blade loads after stall are well above the rotor structural limits (around $C_{m_x}/\sigma = 0.01$ in Fig. 6). However, the power limit is exceeded simultaneously with the loads rise (the transmission limit is $C_p/\sigma = 0.019$ for each rotor). Hence, the power limit is at the lift limit, and the aircraft never actually operates beyond the stall. The constant-power calculations in Fig. 7 best reflect the operating experience. Operating at maximum power, the tilt

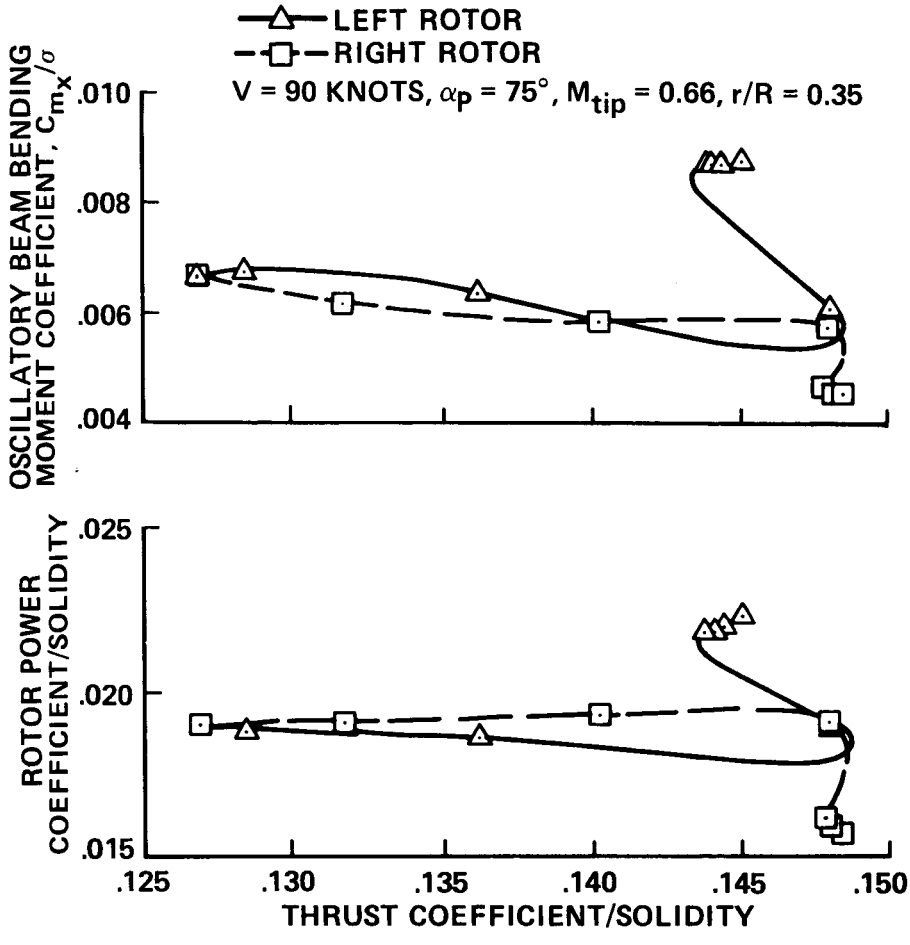

Fig. 7. Calculated XV-15 behavior in steady turns (constant total power).

rotor is climbing at 1.0 g. The vertical-speed rate reduces the wing angle of attack and wing lift, so the rotor must provide more of the total lift (C_T/σ = 0.127). The level-flight power required increases with load factor, but the aircraft is still climbing at the lift limit. At the turn rate corresponding to the level-flight rotor lift limit, the rotor cannot enter the massively stalled operating condition, since the power required would be too large. Hence, the aircraft begins to descend. For higher turn rates, the rotors are operated just before the lift limit, and the increasing descent rate provides an increasing wing angle of attack and wing lift to sustain the larger load factor. The rotor loads remain below the structural limits.

In the present investigation, the rotor lift limit was calculated at only this single operating condition, with the primary purpose of determining whether optimization of the rotor for high-speed performance has a major adverse effect on maneuverability. Then the rotor lift limit and aircraft maneuver requirement were used to select the wing loading in the preliminary design process. By no means are the present designs being optimized for maneuverability. Both wing and rotor need to be considered to define the aircraft limits. For example, with the rotor lift limit just calculated, the maximum load factor at 90 knots

could be increased by tilting the pylon further forward, thereby increasing the wing angle of attack in trimmed flight. The entire subject of tilt-rotor maneuverability deserves more attention to determine both operational and design implications.

6.3. Stability

Whirl flutter is a coupled motion of the prop rotor and the aircraft (typically the wing elastic modes) that becomes unstable at high forward speed. Johnson [8] summarized the phenomenon and the factors controlling it.

With increasing Mach number, the blade lift-curve slope increases at first, which increases the aerodynamic forces involved in whirl flutter, and so has an unfavorable influence on the stability. After lift divergence, the lift-curve slope decreases. If the blade-section Mach number is above the lift-divergence Mach number over a large fraction of the blade tip, the reduction in aerodynamic forces will significantly increase the stability. This phenomenon generally improves the stability as altitude increases, because of the decrease in sound speed. For a high-speed tilt rotor, the phenomenon can produce a minimum in the wing-mode damping at a certain speed, where the helical-tip Mach number is such that the lift-curve slope is maximum. If the wing is not stiff enough, the whirl-flutter boundary is encountered before a helical-tip Mach number increase stabilizes the system.

A gimballed, stiff, in-plane tilt rotor (such as on the XV-15) has negative pitch-lag coupling in cruise, which has a destabilizing influence on whirl flutter. The pitch-lag coupling is produced because the precone is too large for the thrust in propeller operation; hence, there is a negative elastic-coning deflection (see Ref. 8 for a more complete discussion). The magnitude of the coupling can be reduced by various means, including reducing the precone, increasing the control-system stiffness, and increasing the blade droop. This source of coupling can be largely eliminated by reducing the coning stiffness of the hub, as on the V-22 [9].

It is also necessary to ensure the flap-lag stability of the prop rotor, particularly if the stiff, in-plane designs are being used. (Soft, in-plane designs have also been considered [10].) The blade-pitch motion must be included of course, since it is involved in the effective pitch/bending coupling of the blade [8]. Flap-lag stability can be controlled by negative pitch-gimbal coupling [11] (the XV-15 has $-15°$ of δ_3), chordwise offset of the blade center of gravity and aerodynamic center, and the blade stiffness. High inflow and high solidity increase the destabilizing aerodynamic forces. Hence, the blade design for flap-lag stability must be reexamined with high speed tilt rotors.

Figure 8 compares the calculated wing-beam-mode damping ratio with wind tunnel measurements, for a one-fifth-scale semispan aeroelastic model of the V-22 with an early gimballed-hub design [9]. The model

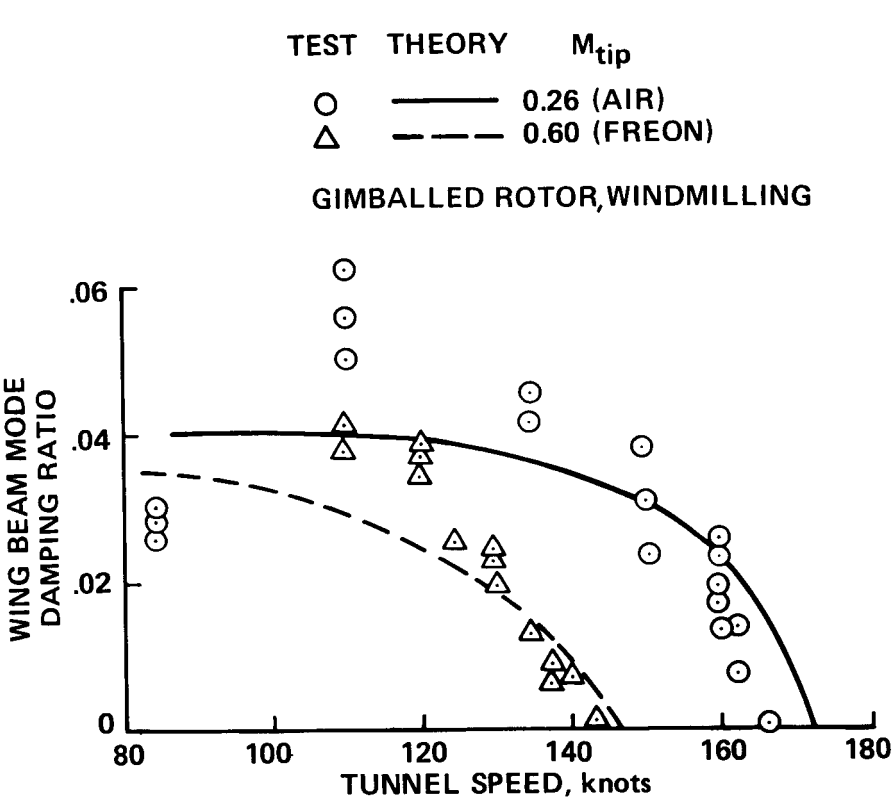

Fig. 8. Whirl-flutter stability of a rotor on a cantilever wing; small-scale wind tunnel test results.

was tested in numerous configurations: a) air and Freon (for full-scale Mach numbers); b) both gimballed and coning hubs; and c) various rotor speeds, blade stiffness, wing stiffness, down-stop stiffness, control-system stiffness, and pitch-flap coupling. Additional correlation is given in Ref. 9.

Figure 9 shows the calculated whirl-flutter stability for the XV-15 in flight. The predicted stability boundary is at 410 knots for constant-power flight (at the transmission torque limit). Note the increase in damping around 400 knots (M_{at} about 0.8) for the level flight case, as a result of the lift-curve slope decrease after lift divergence. This effect is not important here, since the level-flight stability boundary is at 385 knots. The calculations shown in Fig. 9 used the measured values of the XV-15 structural damping, which ranged from 1.5% to 4.0% for the six wing modes. With a structural damping level of 1.0%, the level-flight stability boundary is reduced to 365 knots in the symmetric chord mode (which is stable with the measured damping of 3.5%); and the antisymmetric beam mode is almost unstable as well (measured damping of 2.5%). Correlation of the calculated damping with full-scale wind tunnel and flight measurements for the XV-15 is given in Ref. 5. The calculated stability boundaries are 100 knots or more beyond the maximum speed of the XV-15, so no stability boundary measurements are available.

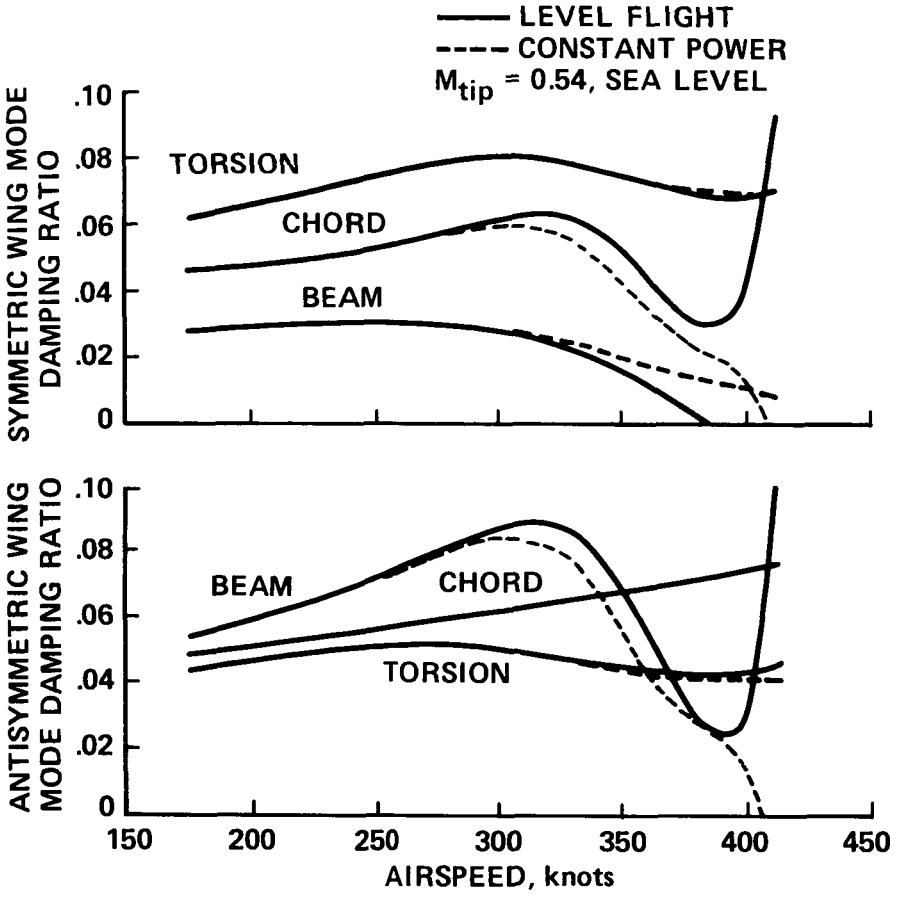

Fig. 9. Calculated XV-15 whirl-flutter stability in flight.

6.4. Design Sensitivity

Using V-22 technology-level assumptions, an initial-design optimization (for minimum gross weight) was conducted, and sensitivities to various design variables were determined. The independent design variables selected were wing loading, wing thickness-to-chord ratio, disk loading, hover- and forward-flight tip speed, number of blades, and rotor solidity. The results of this initial design trade-off study were then used as the starting point of the subsequent aeromechanics analyses.

The sensitivity results also indicated the relative impact of the technology improvements for high-speed tilt-rotor designs. Using the estimated V-22 rotor and wing performance characteristics, the required power for the air-combat vehicle (relative to power required at 300 knots) is presented in Fig. 10 as a function of speed. Airframe-induced and profile-drag power dominate the power requirement over the speed range investigated. Above approximately 340 knots, wing- and rotor-compressibility power requirements become appreciable, and at 400 knots they represent approximately 20% of the required power. Increasing the rotor-drag-divergence Mach number by 10% above the V-22 rotor value would result in a 12% reduction in gross weight for the 400-knot aircraft. Drag sensitivity for V-22 technology-level aircraft indicates

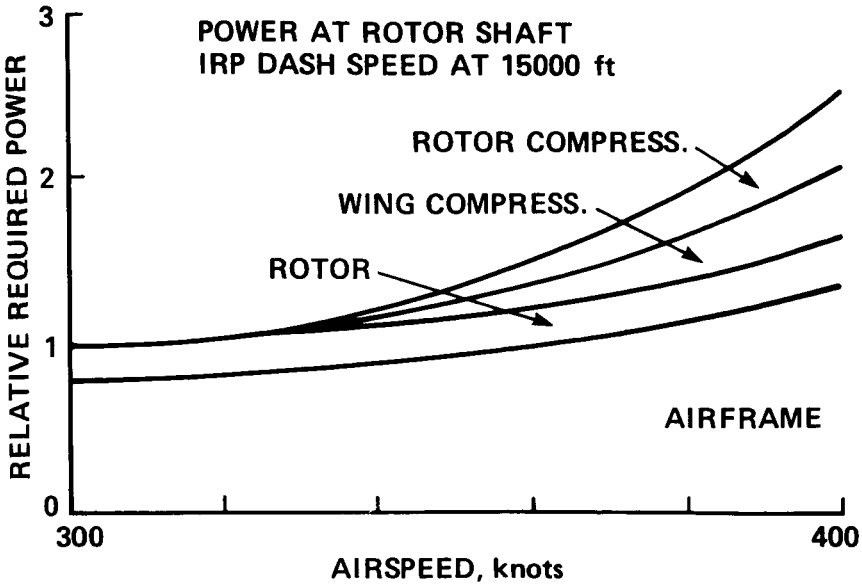

Fig. 10. Calculated sensitivity of required power to flight speed (V-22 technology level).

that a 10% reduction in drag area produces roughly a 4% reduction in gross weight. Eliminating wing-compressibility drag while maintaining the thick airfoil section can result in a 10% gross-weight reduction. Because of the pronounced sensitivity of the required power, which determines engine size, fuel weight, and vehicle gross weight, feasible high-speed tilt-rotor designs will depend on low airframe drag configurations, coupled with advanced wing and rotor airfoil sections optimized for minimum compressibility penalties. Unlike Fig. 10, the power required for a high-speed aircraft will then show only small compressibility losses at the design speed.

The required power presented in Fig. 10 does not include momentum-loss terms (i.e., suppression cooling flow and negative tailpipe thrust) since these power increments are more engine-cycle-dependent. For high-speed tilt-rotor designs, large, negative tailpipe thrust can have a significant impact on the vehicle gross weight and resulting performance. Consequently, only engines with higher nozzle pressure ratios were considered in the advanced-technology designs.

7. ADVANCED TECHNOLOGY AND OPTIMIZATION

The starting point for the present investigation are the XV-15 and V-22 technologies just described. The rotor aerodynamic design, which determines the performance and lift limit, is examined. Advanced-technology airfoils are considered, and the blade aerodynamic design is optimized for high-speed cruise. An advanced-technology wing airfoil is considered, to minimize airframe drag at high Mach number.

In the matter of aircraft dynamics design, an advanced-technology hub is considered, and the wing stiffness is optimized for high speed.

It must be recognized that at the design stage of this investigation, no detailed information about the structural and inertial properties of the rotor and airframe is available. Hence, the dynamic stability were not calculated with the same accuracy as was the aerodynamic performance.

7.2. Advanced Airfoils

For high speed prop-rotor designs, airfoils with high-drag-divergence Mach number are needed. Advanced airfoils are available that have already been tested two dimensionally, and that offer significant improvements compared to the airfoils on the XV-15 and V-22. Figure 11 shows the key airfoil characteristics considered and the distribution of the airfoils along the rotor-blade span. The XV-15 and V-22 blades are described in Ref. 7. The sharp jumps in characteristics shown in Fig. 11 are simply the edges of the aerodynamic analysis panels in the analysis; the actual blade has more gradual transitions between airfoil sections. Note that at the blade tip the spanwise extent of the thin airfoils with high drag divergence Mach number has been increased for the advanced airfoils. As a result, the maximum lift coefficient is lower with the advanced airfoils--the expected compromise for a high-speed design. The lift divergence Mach number (where the lift-curve slope begins to decrease) is about 0.125 less than the drag divergence Mach number for all these airfoils.

Figure 12 shows the calculated influence of advanced airfoils on the prop-rotor performance. The influence follows directly from the

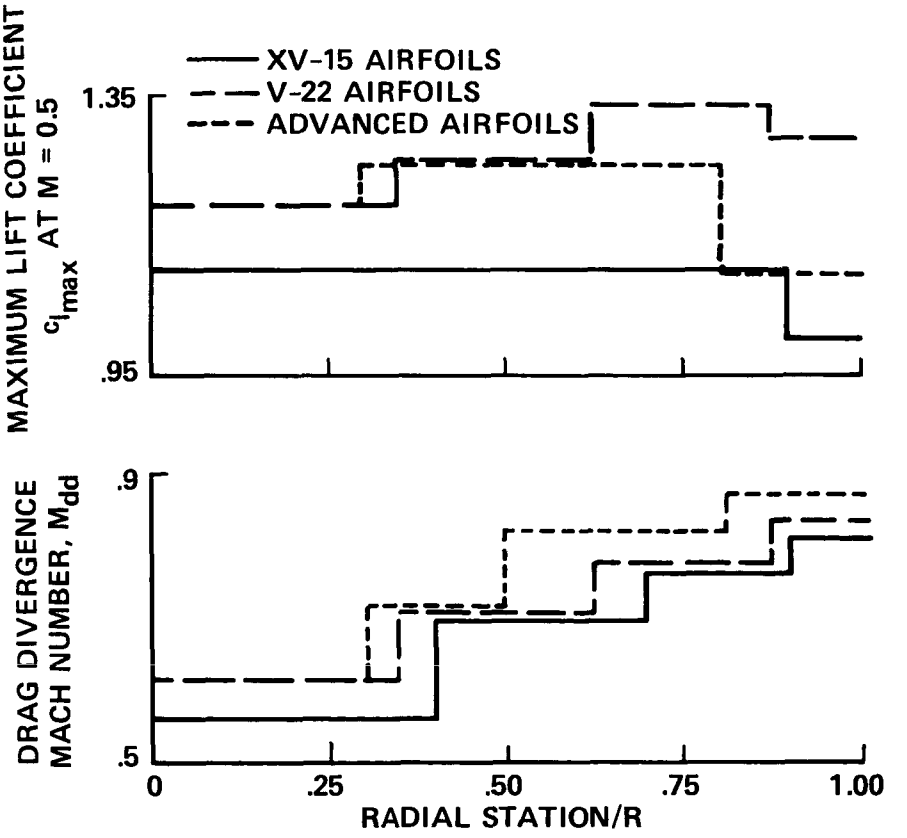

Fig. 11. Airfoil characteristics as a function of blade-radial station.

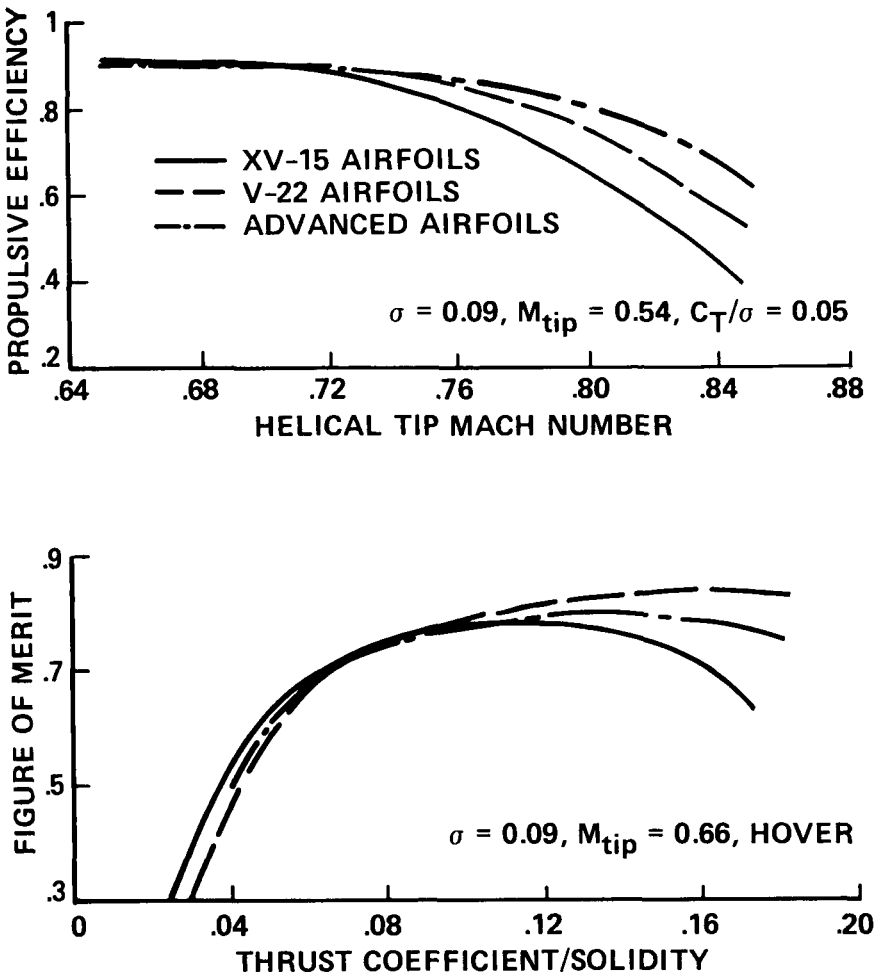

Fig. 12. Calculated influence of advanced airfoils on prop-rotor performance.

drag-divergence and maximum lift characteristics shown in Fig. 11. The higher-drag-divergence Mach number of the newer airfoils improves the propulsive efficiency significantly, allowing the rotor to operate at higher tip speeds in cruise. Below drag divergence, the influence of Mach number on the efficiency is small. The hover figure of merit is not as good with the advanced airfoils as with the V-22 airfoils, because of the lower maximum lift coefficient at the tip. The difference in figure of merit is minimized by the high disk loading; however, hover power is not a design driver for a high-speed tilt rotor in any case.

Table 2 shows the calculated influence of the advanced airfoils on the tilt-rotor maneuverability, in terms of the rotor lift limit in turning flight. This limit is determined by the blade stall characteristics, and hence shows the same trends with airfoils as does the hover figure of merit.

Table 2. Calculated influence of advanced airfoils on tilt-rotor lift limit in turns at 90 knots and 75° pylon angle (σ = 0.09, M_{tip} = 0.66).

	At maximum rotor lift	
Turn rate, deg/sec	C_T/σ	
XV-15	16.4	0.150
V-22 airfoils	21.3	0.185
Advanced airfoils	19.8	0.173

7.2. Advanced Hub

The whirl-flutter stability boundary is sensitive to the airframe mode shapes. Since detailed information about the airframe structural dynamics is not available at an early design stage, the XV-15 airframe modes were used for the high speed designs. A structural damping value of 1.5% was used for all modes; this value is the lowest damping found on the XV-15. The natural frequencies of the XV-15 airframe modes were taken as the starting point for developing the high-speed designs.

The V-22 hub configuration offers improved stability relative to the XV-15 [9]. In the present work a coning hub is considered for the high speed designs. This hub represents attainable advanced technology (since it is similar to the V-22 hub), but no attempt has been made to find an optimum hub configuration. In the advanced hub, the gimbal is retained and a flap hinge is introduced on each blade, at 3.5% radius. The steady flap moment must be zero at this coning hinge; hence, the negative pitch-lag coupling is reduced, which has a stabilizing influence on whirl flutter.

With the higher solidity and higher flight speeds of the designs to be developed here, the rotor flap-lag stability must be examined. To achieve flap-lag stability, the kinematic pitch-cone and pitch-lag coupling are set to zero (retaining the -15° of pitch-gimbal coupling); and the blade center of gravity and elastic axis are shifted forward by about 5% chord relative to the aerodynamic center. Negative pitch-cone coupling and positive pitch-lag coupling would help, but would be difficult to obtain. The aerodynamic-center shift is taken as a fixed fraction of the rotor radius, and so is a smaller fraction of the chord for the higher solidity rotors. The aerodynamic-center shift also has a significant stabilizing influence on the whirl flutter.

Figure 13 shows the calculated influence of the advanced airfoil and hub on the stability of the critical wing modes. The delay of compressibility effects with the advanced airfoils means that the Prandtl-Glauert rise in lift-curve slope extends longer and higher. The resulting increase in rotor aerodynamic forces has an unfavorable influence on wing-mode stability. However, the favorable influence of the advanced hub more than compensates for the airfoil influence however, so there is a net gain produced by the new technology [9]. Note that with the advanced airfoils and hub, the damping actually increases beyond 400 knots (M_{at} about 0.8).

To maintain flap-lag stability with the larger solidity of the high-speed designs, it was also necessary to increase the blade bending stiffness and control-system stiffness. The higher blade frequencies also have a stabilizing influence on whirl flutter, increasing the damping level of all the wing modes.

The objective of these parameter changes was only to find a design that met the stability requirements. There is a clear opportunity for an effort to optimize the rotor-blade and hub designs, with emphasis on simplicity, low weight, and stability.

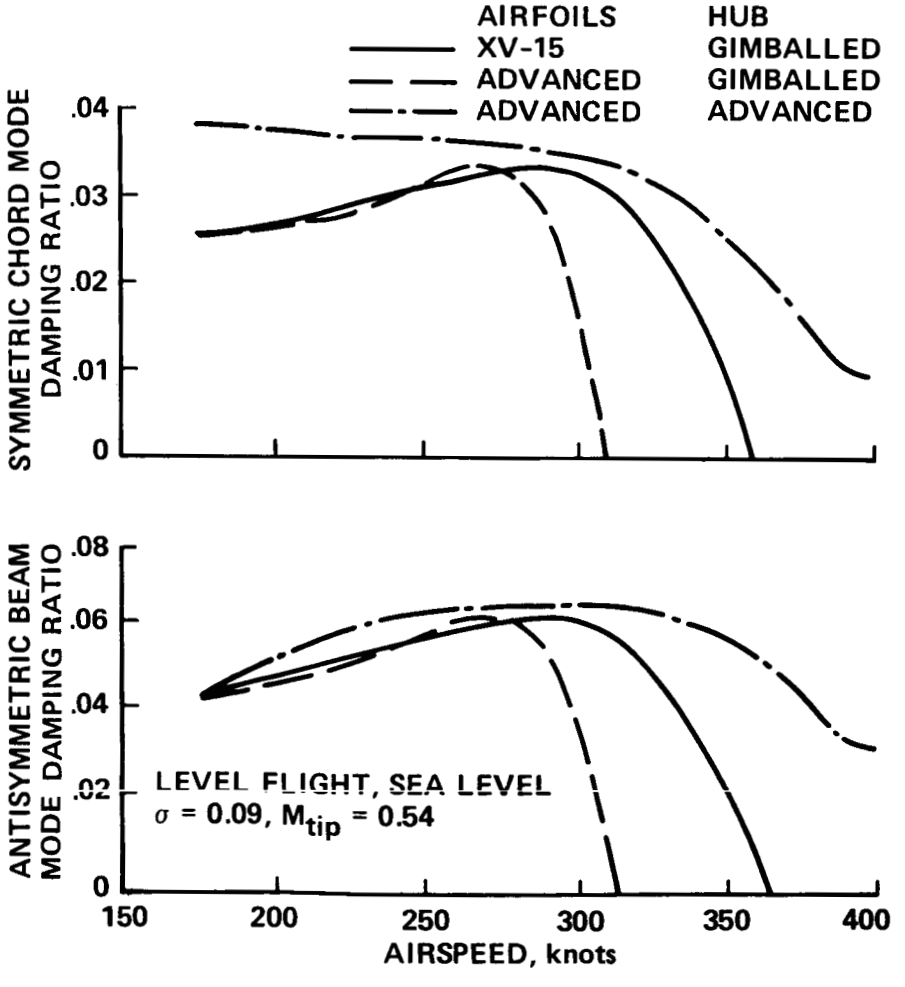

Fig. 13. Calculated influence of advanced airfoils and hub on tilt-rotor stability.

7.3. Airframe Weight

Where applicable, advanced-technology factors are applied to the component weight to reflect the expected weight reduction resulting from the application of advanced materials. For the purpose of this study, both primary and secondary structures are assumed to be constructed of composite materials. This type of material typically provides approximately a 20% weight reduction compared to similar metal designs. The weight technology factors used here are representative of the level chosen for the V-22 design.

7.4. Airframe Drag

As is true for all high-speed aircraft, profile drag reduction can result in significant reduction of installed power and gross weight. State-of-the-art design practice should be sufficient to produce efficient airframe designs for the 375 knot civil transport (0.6 Mach number at 20,000 ft). The drag levels selected for the 46-passenger tilt-rotor transport are representative of modern turboprop commuter aircraft. Pessimistic nacelle drag levels were assumed for the civil transport in this study, representing approximately 33% of the total airframe drag area. The drag levels for the 400-knot air-combat tilt rotor are based on the original design for the XV-15, which had smaller and more contoured gear pods than the final design. External mission equipment (such as a gun turret, FLIR, and TADS) were assumed to add 1.36 ft^2 of drag area. However, conformal or internal missiles stores will be required to meet the desired airframe drag levels. This requirement could impact the overall configuration layout integration, and more detailed design analysis may be needed. For both high-speed tilt-rotor designs, the assumed profile drag levels are somewhat conservative and no assumptions are made regarding dramatic drag-reduction technology.

With aeroelastic wing stiffness requirements dictating thick wing sections for minimum wing weight, a high speed tilt rotor can expect to incur some level of wing wave drag. The drag rise for the 23%-thick XV-15 wing section begins at Mach 0.575 for a wing-lift coefficient of 0.25. The associated drag divergence Mach number is approximately 0.625. For the civil transport flying at Mach 0.6, the wing wave drag will have minimum impact. However, for the 400-knot (0.65 Mach) air-combat tilt rotor, wing-compressibility effects are more pronounced.

Raymond Hicks of the Advanced Aerodynamics Concepts Branch at Ames Research Center conducted a study of reducing the upper-surface shock on the 23%-thick airfoil at Mach 0.65 and at lift coefficients from 0.2 to 0.4. Using a two-dimensional transonic, viscous-flow code [12], and beginning with the NASA Langley Research Center 17%-thick Medium-Speed Airfoil MS(1)-0317 [13] contour, the upper- and lower-surface coordinates were modified to produce the rather blunt MS23N airfoil section. Figure 14 shows the airfoil contours and the upper- and lower-surface pressure coefficients at the design operating point.

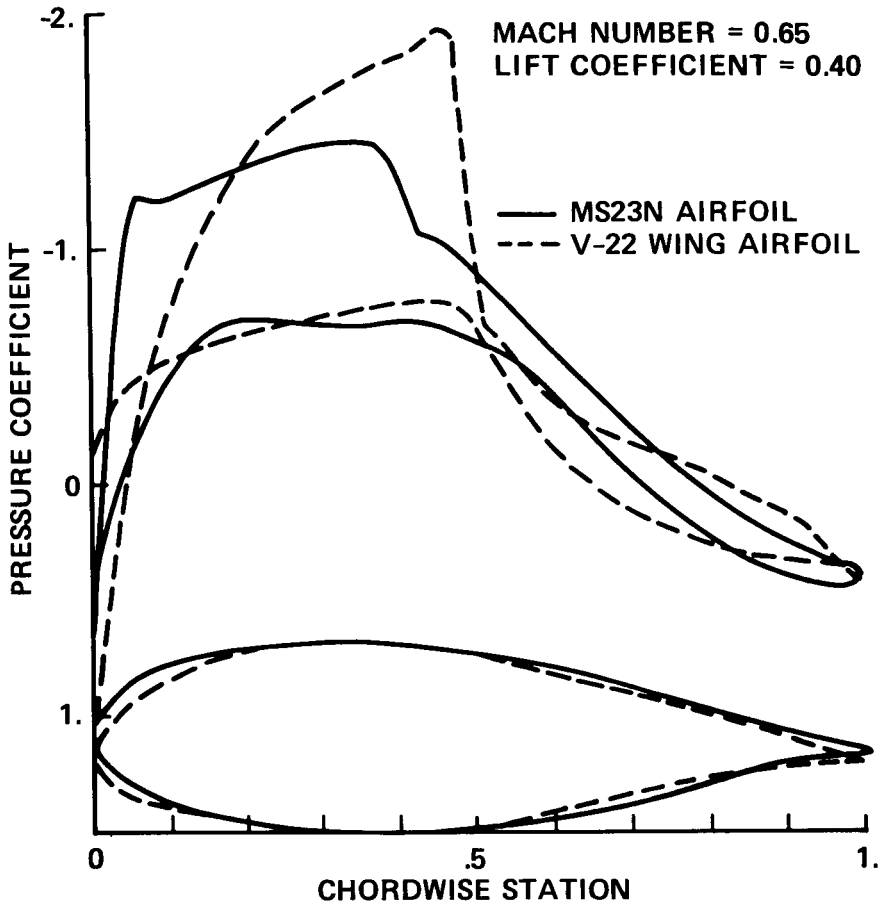

Fig. 14. Calculated two-dimensional pressure coefficients for wing airfoils.

For comparison, the calculated pressure distribution for the 23% V-22 wing airfoil at the same operating condition is shown in the figure. A wave-drag-coefficient reduction of 0.0070 is estimated to occur with the MS23N airfoil, with only modest increase in the airfoil-profile drag coefficient.

Wing-compressible drag rise predicted by the two-dimensional transonic code was compared with small-scale wind tunnel test results for the complete XV-15 configuration. The two-dimensional code predicted drag-rise levels less than those measured in the wind tunnel. The difference is assumed to arise from three-dimensional and interference drag effects. For the advanced-technology study, only the wing component of the wave drag was assumed to be eliminated with the application of the advanced MS23N airfoil. Hence, the transonic interference increment was retained in the vehicle drag estimation at high speed.

7.5. Blade Aerodynamic Optimization

The aeromechanics analysis was used to optimize the rotor and airframe parameters for high-speed operation. Blade taper was not used, since it was found to improve hover performance at the expense of cruise

performance. When the blade structural loads and weight are considered in the detailed design stage, blade taper could be examined again.

Blade twist is the remaining parameter to optimize. For cruise operation, a small, positive, lift coefficient all along the blade is desired. The requirement for a propeller blade, which operates at a higher lift coefficient, would be more complex. The large blade area of the prop rotor means that the lift coefficients in cruise are small, so the drag produced by lift is not large. The key consideration is the avoidance of compressible-drag rise all along the blade. For the entire blade to be at the same section angle of attack, a twist variation equal to $\tan^{-1}(V+v)/\Omega r$, is required (about equal to $\tan^{-1} V/\Omega r$ since v/V is small). Hence, the optimum twist depends on $V/\Omega R$. A two-piece, linear-twist variation is a good approximation to the nonlinear distributions used, and as a two-parameter model is convenient for the optimization analysis. The inboard slope and outboard slope are joined at radial station $r = 0.5$. (Effectively the transition between $r = 0.45$ and $r = 0.55$ was smooth, since there was no aerodynamic analysis point near $r = 0.5$.) At $V/\Omega R = 1.1$, the inboard/outboard slopes corresponding to uniform lift coefficient are approximately -51°/-35°. Note that this aerodynamic twist refers to the zero-lift angle of the airfoil section.

Figure 15 shows the calculated influence of twist on the performance of the prop rotor. The inboard and outboard slopes are varied for $V/\Omega R = 1.1$. At high Mach number, the twist has a significant effect on the cruise efficiency. The optimum twist delays the degradation of performance associated with the compressible-drag rise. There is only a small reduction of hover efficiency with the twist optimized for high-speed cruise (although the hover efficiency might be more sensitive to twist with a nonuniform inflow analysis). The optimum twist for cruise performance is about -48°/-34°. This optimum twist is less of a twist than is required for the uniform-lift coefficient; it is beneficial to load the tip more and keep the lift small at the root.

The XV-15 blade has a nominal twist rate of about -60°/-26° [7], which is more like -63°/-28° when the airfoil zero-lift angles of attack are included. The V-22 has a twist rate of about -61°/-29° [7] (a better approximation inboard is given by -75°, extending only to $r = 0.42$). Hence, as expected, the high speed designs considered here require a larger outboard twist rate.

Figure 16 shows the calculated performance of the prop rotor with blade aerodynamics optimized for high-speed cruise: advanced airfoils, no taper, and the optimum twist (-48°/-34°). The optimum twist has little influence on either the rotor-lift limit (maneuver capability) or the high-speed stability.

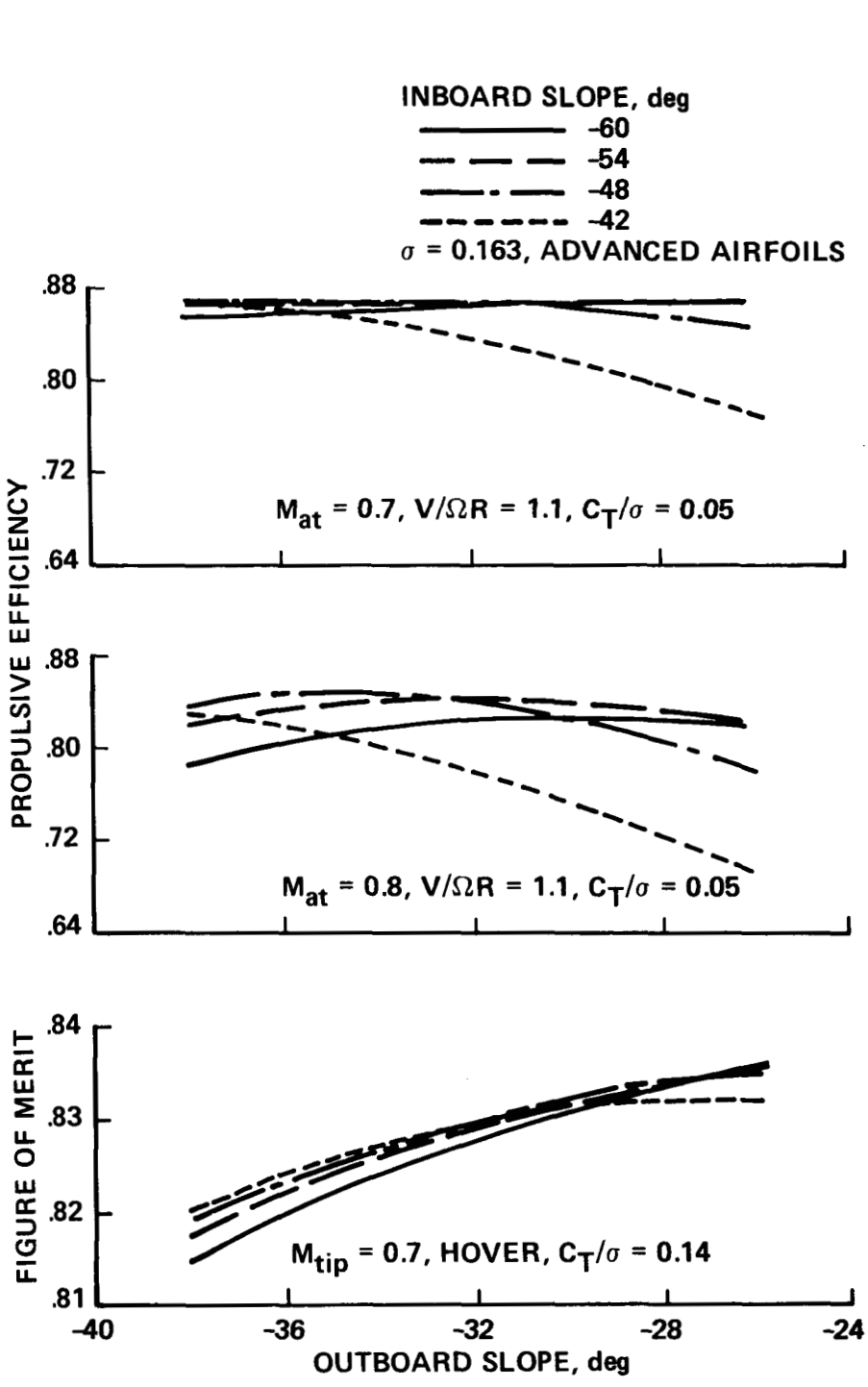

Fig. 15. Calculated influence of blade twist on prop-rotor performance.

7.6. Wing-Stiffness Optimization

With the prop-rotor aerodynamics optimized for high-speed performance and using the advanced hub, it is now necessary to determine the minimum wing stiffness (and hence minimum wing weight) required to ensure stability at high speed. For the present purposes the whirl-flutter criterion is that the stability boundary be beyond 500 knots (1.25 times the design speed).

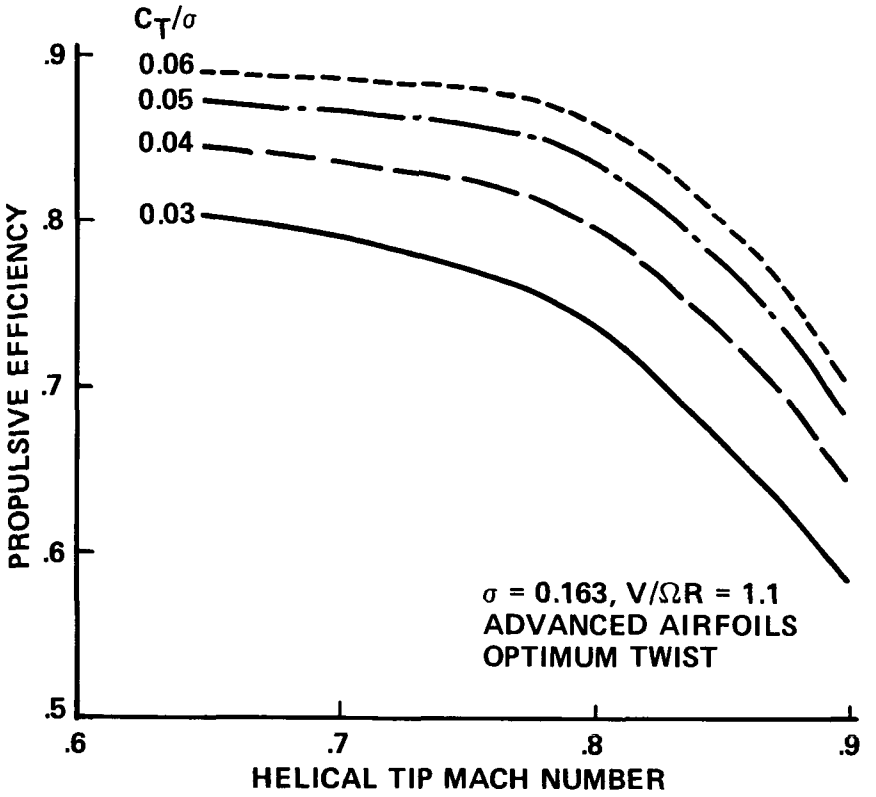

Fig. 16. Calculated propulsive efficiency of prop-rotor with advanced airfoils and optimum twist.

Figure 17 shows the influence of the wing stiffness on the whirl-flutter stability. For the baseline case (XV-15 wing frequencies, 550-ft/sec tip speed) the symmetric chord mode is unstable at 376 knots and the antisymmetric beam mode at 415 knots. The wing frequencies were therefore increased by 10% (a 21% increase in wing stiffness; the wing torsion modes are not critical, so their frequencies were increased by only 5%). For this stiffer configuration there is a minimum in stability around 415 knots (M_{at} about 0.8, where the lift-curve slope is largest). Enough wing stiffness to produce an adequate level of damping at 415 knots is required; then the aircraft is stable to 500 knots. For this study, the advanced hub design has contributed substantially to achieving the required stability at 415 knots. The rotor tip speed is varied in the preliminary design process, so it is necessary to define a criterion for all tip speeds. By specifying the wing stiffness in terms of frequencies per revolution, the stiffness will increase with an increase in the tip speed. Figure 17 shows this procedure to be an adequate approach; with the frequency-per-revolution criteria, the stability is improved for 650-ft/sec tip speed. Note that a minimum in the damping then occurs around 360 knots, again at about $M_{at} = 0.8$.

Table 3 gives the wing-stiffness criteria used for the high-speed designs. The frequencies of the XV-15 and V-22 symmetric wing modes are given for comparison. The high-speed criterion should be conservative, yet stiffer than the XV-15 and V-22. A per-revolution criterion implies

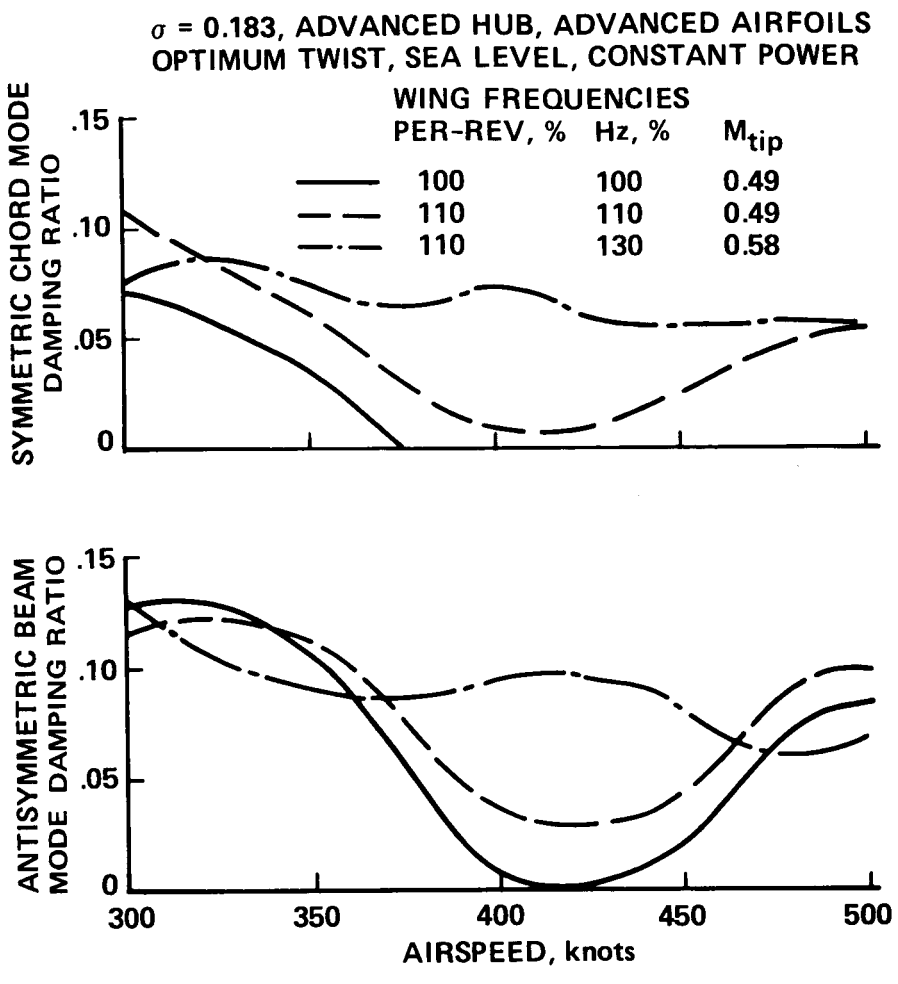

Fig. 17. Calculated influence of wing stiffness on tilt-rotor stability.

Table 3. Wing stiffnesses (symmetric modes)

	Tip speed, ft/sec	Ω, Hz	Frequencies/rev		
			Beam	Chord	Torsion
XV-15 TRRA	600	7.64	0.45	0.86	1.07
V-22 Osprey	662	5.54	0.53	0.80	0.91
High-speed criterion	all	---	0.53	1.04	1.23

that the stiffness increases with tip speed. The criterion is based on an extreme case (sea level flight and large solidity).

7.7. Preliminary Design Optimization

Using the optimized rotor design, the aeroelastic stability criteria, and the redesigned wing airfoil, the two tilt rotor configurations were then redesigned. The design parameters selected for the optimization process were disk loading, wing loading, and hover- and cruise-mode tip speed. Using the new wing airfoil section, the wing thickness-to-chord ratio was held fixed at 23%. With no wave-drag penalty for this thick airfoil, the wing stiffness requirements can be met at the minimum wing weight.

Based on results obtained in the initial design optimization, the number of rotor blades and the hover blade loading were held fixed. A four-bladed rotor design was selected. For fixed total-blade area, a smaller blade chord results as the number of blades increases, producing a higher aspect-ratio blade and lower rotor-control weight. The hover design C_T/σ also has a strong impact on the vehicle design, with the gross weight decreasing with an increase in blade loading. For fixed disk loading, as C_T/σ is increased, the rotor solidity decreases, resulting in reduced blade area. With the rotor sized for high-speed cruise, the lower blade area results in lower rotor profile drag, and hence a higher rotor efficiency. This impact cycles through the design to produce smaller engine size, less fuel weight, and lower vehicle weight. The lower solidity also permits lower rotor weight and rotor-control weight. For this study, the hover C_T/σ was limited to a value of 0.125, somewhat lower than the design value for the V-22. This imposed limit results in a weight penalty for both the civil transport and the air-combat tilt-rotor designs. However, the larger blade area would allow future growth in vehicle weight and would provide improved low speed maneuverability for the air-combat design.

7.8. Disk Loading Selection

For tilt-rotor configurations, the rotor-disk loading is a dominant design variable. With the hover C_T/σ fixed, the rotor solidity becomes proportional to the disk loading, although the blade area remains constant (decreased radius with higher disk loading is offset by increased chord). The disk loading also determines the rotor radius, which in turn defines the wingspan for tilt-rotor designs. Wing weight and wing-induced drag are in turn functions of wingspan. The disk loading will also determine the rotor rotational speed for a fixed tip speed; the rotor rpm in turn influences the engine and transmission sizing, and also influences the wing-weight through the wing-stiffness criteria (in terms of dimensionless frequencies). Thus,

there is a strong coupling of the rotor design and the airframe characteristics through rotor-disk-loading variations.

Disk loadings from 15 to 35 lb/ft^2 were examined for the present study. For a specified design speed, the airframe parasite power and rotor power are approximately constant and independent of disk loading (rotor-induced power at high speed is small, and fixed-blade area results in roughly constant rotor profile power). Thus, only the wing-induced power will vary with disk loading. In the lower disk-loading range (15 to 20 lb/ft^2), the large-diameter rotor results in high wingspan, providing lower wing-induced drag. Even for the high-speed design applications, the wing-induced drag is 5% of the total drag for the air-combat aircraft, and 20% for the civil transport, with wing-lift coefficients of 0.2 and 0.4, respectively (determined here by the high wing loading selected in the optimization process). The lower induced-drag level in turn results in lower engine power required; hence, less fuel is burned. With rotor-blade area fixed by the hover C_T/σ, the lower disk loadings also resulted in reduced blade chord, giving it a lighter rotor-control weight. These benefits for the large rotor-radius design are offset by higher wing weights (caused by a large wingspan), higher rotor and hub weights, and increased transmission weights (with rotor tip speed being held constant). Also, the reduced drag is offset somewhat by a smaller rotor propulsive efficiency, since lower drag and fixed hover C_T/σ imply a reduced cruise C_T/σ. For initial increases in disk loading, these benefits outweigh the penalties. Further increases in disk loading result in even higher wing-induced drag, with engine power and fuel weight increases overcoming the flattening trend in increased rotor efficiency with higher cruise C_T/σ. The net result is a minimum vehicle gross weight at a disk loading in the the mid 20-lb/ft^2 range.

Gross weight is relatively insensitive to disk loading for both the civil transport and air-combat tilt rotors, changing only 5% in the 15- to 35-lb/ft^2 range studied. If other mission or design constraints were imposed which would drive the design to a higher or lower disk loading, little change in the total vehicle weight would occur. For example, if direct operating cost were considered for the civil tilt-rotor, somewhat lower disk loadings might result, reflecting the lower acquisition cost for a smaller engine.

To increase wing aspect ratio for fixed disk loading, increasing the clearance between the rotor tip and fuselage

was investigated. The results led to increased wing weights with increased wingspan, and hence higher vehicle gross weight. At the high end of disk loadings studied (30-35 lb/ft^2), wing extensions outboard of the nacelle were investigated. These extensions would increase the span, hence lower the wing-induced drag. However, the benefits of higher span were negated by increased weight and wetted area, nacelle strengthening for load carrythrough, and reduction in Oswald efficiency factor. Only at high disk loadings did wing extensions show any net advantage.

7.9. Wing-Loading Selection

With the wingspan defined by the disk loading (which determines the rotor radius), variations in wing loading change wing chord only. At low wing loading, the wing chord will be large, resulting in higher wetted area (hence higher wing-profile drag) and higher power required. The large chord, however, will provide larger physical wing thickness, and hence reduced wing weight. As wing loading is increased, wing-profile drag is reduced, (wing-induced power remains constant since the wingspan is fixed), but wing weight grows dramatically with reduced chord. Again, for a fixed disk loading, there is a local minimum in gross weight versus wing loading. For the air-combat tilt rotor, the wing loading was limited to 90 lb/ft^2 by low speed maneuverability considerations, but with the local minimum at 100 lb/ft^2 the resulting gross-weight penalty was minor.

7.10. Hover Tip-Speed Selection

With the hover C_T/σ fixed for both tilt-rotor designs, changes in hover tip speed produce blade area and solidity changes (for fixed disk loading). As tip speed is increased, blade area is reduced, providing high rotor propulsive efficiency and lighter rotor weight. This trend is offset by somewhat higher engine power (from increased ratio of hover to cruise engine rpm) and an associated increase in transmission weight. The gross-weight trend is very flat, with a minimum occurring at 785 ft/sec for both the civil-transport and air-combat designs. If hover noise is a concern for the civil-transport tilt rotor, moderate reductions in hover tip speed will result in only modest gross-weight penalties.

7.11. Cruise Tip-Speed Selection

For tilt-rotor configurations, the rotor tip speed is reduced during airplane-mode operation, giving a better rotor operating point at cruise thrust levels. For high-speed tilt-rotor applications, reduced tip speed will also

be required to minimize rotor compressibility effects. Reducing the tip speed in cruise requires the engine to operate at a lower speed, resulting in off-design performance and associated penalties. The aeroelastic stability requirements, based on dimensionless wing frequencies (airframe-mode frequency divided by rotor-rotational speed), couple the tilt-rotor wing weight to the rotor cruise speed, since the required wing-box, cross-sectional area decreases with lower rotor speed. Thus, the rotor tip speed impacts the vehicle characteristics through rotor and engine performance, wing stiffness, and weight.

As the rotor tip speed is reduced, the rotor efficiency improves because of the improved loading and reduced helical-tip Mach number. Wing weight also decreases with lower rotor speed. With further tip-speed reductions, the engine off-design penalties and increased transmission weight (higher torque) tend to reverse the declining gross-weight trend. As an added degree of conservatism, the tip speed used with the wing aeroelastic-stability criterion was limited to 600 ft/sec; hence, wing weight was not further reduced at lower tip speeds. As with the other design variables, a minimum in vehicle gross weight versus tip speed occurred for both tilt-rotor designs.

8. HIGH SPEED DESIGNS

8.1. Design Description

The principal design parameters, weights, and drag characteristics for the high-speed tilt-rotor designs are given in Tables 4-6. Three-view drawings of the two designs are shown in Figs. 18 and 19. The performance, stability, and maneuverability were calculated for both final designs. Figure 20 shows the calculated performance in hover and cruise. In cruise the design-operating condition is about $C_T/\sigma = 0.05$, where the propulsive efficiency is 0.853 (for $V/\Omega R = 1.1$). In hover the design operating condition is about $C_T/\sigma = 0.14$, where the figure of merit is 0.830. The calculated stability shows all airframe modes stable to at least 500 knots. The stability is better than that shown in Fig. 17 because of the smaller solidity of the final designs. The calculated lift limit in turns at 90 knots and 75° pylon angle is $C_T/\sigma = 0.174$ for both aircraft (determined primarily by the rotor airfoils--see Table 2). For this pylon angle, the wing lift coefficient is about 1.3 at the rotor-lift limit. Assuming that the pylon angle is such that the wing is operating at a lift coefficient of 1.9 (a reasonable maximum with flaps up), these aircraft could achieve a load factor of 1.9 g at 90 knots. For a further increase in maneuver capability,

Table 4. Tilting prop-rotor aircraft parameters

	Current designs		High-speed designs	
	XV-15 TRRA	V-22 Osprey	Civil transport	Air-combat fighter
Design gross weight, lb	13000	39500	39400	16300
Rotor radius, ft	12.5	19.0	15.1	10.4
Wingspan, ft	32.2	45.0	40.6	26.3
Engine power, hp	1400	6150	5423	4092
Cruise transmission limit, hp	2400	7040	6320	5440
Number of blades	3	3	4	4
Rotor solidity	0.089	0.105	0.159	0.155
Hover tip speed, ft/sec	740	790	785	785
Cruise tip speed, ft/sec	600	662	540	610
Outboard twist rate, deg	-26	-29	-34	-34
Rotor airfoils	64-series	XN-series	Advanced	Advanced
Rotor hub type	Gimbaled	Coning	Advanced	Advanced
Wing airfoil	64A223(Mod)	SF821201	MS23N	MS23N
Wing loading, lb/ft^2	77	103	110	90
Disk loading, lb/ft^2	13.2	17.4	27.5	24.0
Blade loading, lb/ft^2	149	166	173	155
Wing aspect ratio	6.1	5.3	4.6	3.8
Fuselage drag coefficient	0.056	0.063	0.041	0.049
Power loading, lb/hp	4.6	3.2	3.6	2.0
Cruise efficiency, VW/P	5.0	5.8	7.1	3.7

the blade loading or wing loading must be decreased. For example, the air-combat fighter could achieve 2.2 g at 90 knots with the blade loading decreased by 12% and the wing loading decreased (or the wing maximum lift coefficient increased) by 22%.

Reflecting the high-speed cruise requirement coupled with minimum hover considerations, both high-speed designs incorporate fairly high disk loadings compared to those of existing rotor craft. This higher disk loading also results in higher rotor solidity and modest wing-aspect ratios. Although designed for a 400-knot capability, the air-combat vehicle spends most of its mission at lower speed escorting the troop transport. The design optimization of the air-combat tilt rotor was thus influenced by low-speed performance considerations. The optimized disk loading tends toward lower values when compared to the civil transport, which flies most of its mission at the design cruise speed.

Table 5. Component weights of high-speed tilt-rotor designs

	Civil transport		Air-combat fighter	
	lb	%	lb	%
Wing	1457	3.7	605	3.7
Rotor and hub	2129	5.4	812	5.0
Empennage	528	1.3	258	1.6
Body and landing gear	4724	12.0	1782	10.9
Engine section	558	1.4	451	2.8
Engine and subsystems	1945	4.9	1935	11.9
Transmission	3000	7.6	1648	10.1
Fuel system	435	1.1	404	2.5
Controls	2083	5.3	1323	8.1
Fixed equipment	7239	18.4	2372	14.6
Fuel	5681	14.1	3233	19.8
Fixed useful load	598	1.5	269	1.7
Payload	9000	22.9	1200	7.4
Gross weight	39378	100.0	16292	100.0

Table 6. Airframe drag of high-speed tilt-rotor designs (airplane configuration)

	Civil transport		Air-combat fighter	
	ft^2	%	ft^2	%
Body, empennage, gear pod	6.41	43	3.40	38
Wing	3.12	21	1.60	18
Nacelle	5.30	35	2.50	28
External systems	---	--	1.36	15
Total drag area	14.83	100	8.86	100

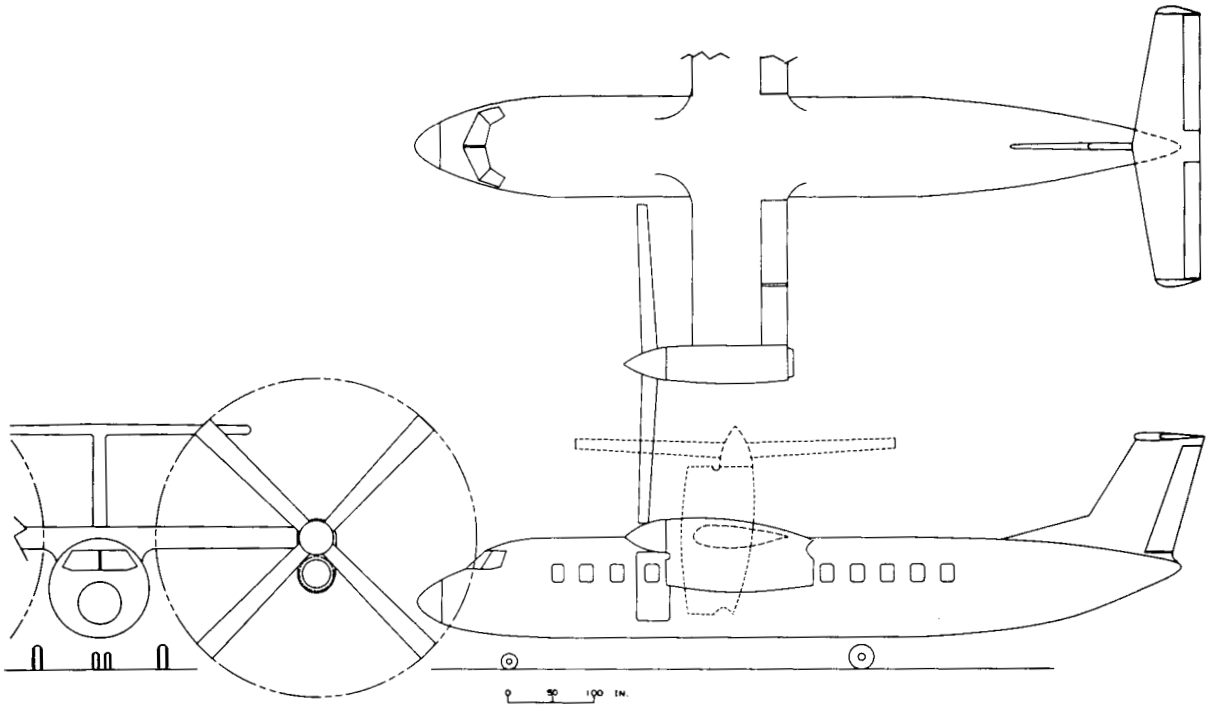

Fig. 18. Three views of the high-speed, civil-transport design.

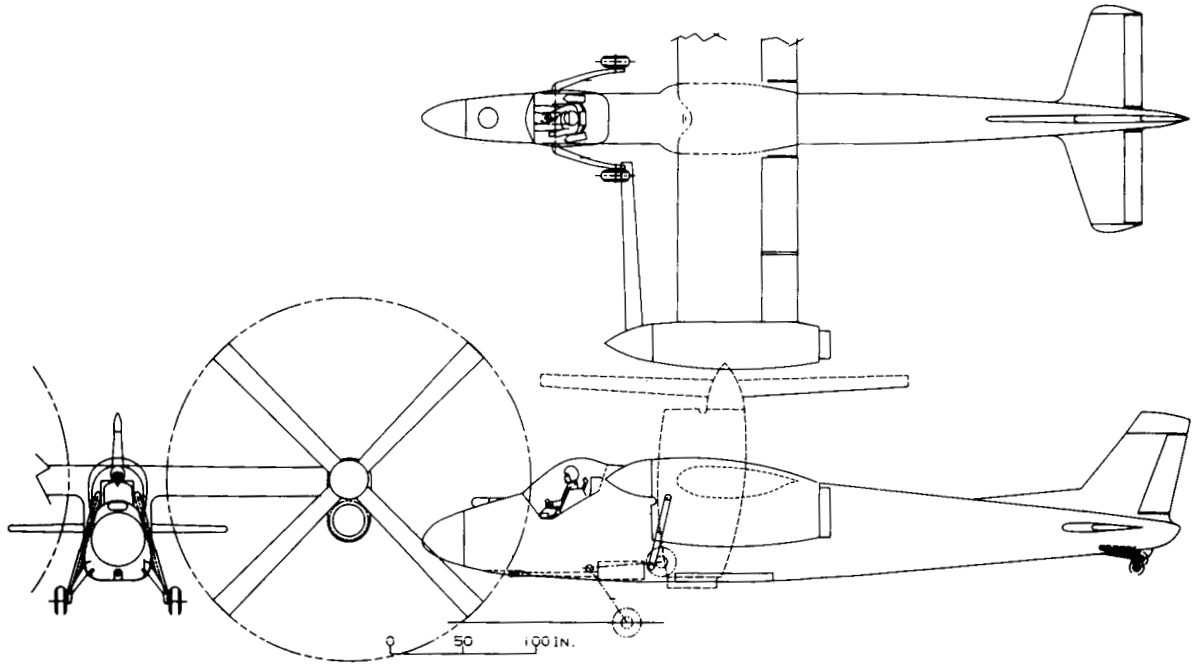

Fig. 19. Three views of the high-speed, air-combat-fighter design.

Wing-induced drag at the lower mission speed biased the disk loading to a relatively lower value compared to higher-speed applications. The cruise tip speed for both designs has roughly the same helical-tip Mach number (0.80), which places the design near the knee of the rotor compressibility curve (Fig. 16). The power loading, calculated from the engine's sea level static power at 100% rpm, is relatively low because of the combination of high speed and the operation of the engine at

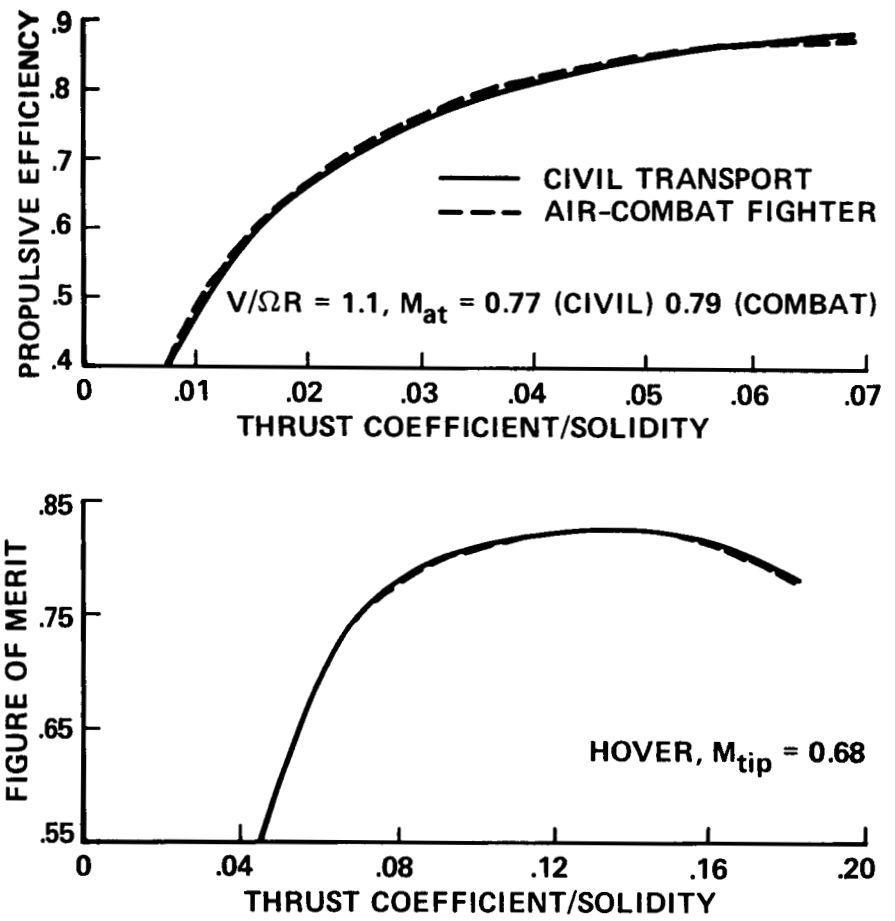

Fig. 20. Calculated propulsive efficiency and figure of merit for the high-speed tilt-rotor designs.

reduced rpm in cruise. The power loading of the air-combat design is half that of the civil transport, reflecting the power required for high speed at low altitude. With both designs driven overall by the high-speed requirements, the engines sized for cruise have ample power for hover and low speed. The cruise efficiency, VW/P, is the product of the prop-rotor propulsive efficiency and the aircraft lift-to-drag ratio. For the tilt rotor, VW/P is calculated from the cruise power (transmission limit). The cruise efficiency of the air-combat design is half that of the civil transport.

Sensitivity studies about the optimum design point were conducted to determine the vehicle gross-weight dependence on the assumed technology level. The results are presented in Table 7. The most pronounced sensitivity is in added weight (such as additional payload). However, the resulting gross-weight variation (15 to 19%) is more comparable to fixed-wing sensitivity than to that of typical vertical-takeoff-and-landing (VTOL) aircraft. Rotor efficiency and airframe-drag sensitivity are less than 1:1 in gross weight. Wing stiffness and wing thickness (for reduced wave drag, if needed) show little impact. The overall sensitivities are more pronounced for the higher-speed air-combat design. Finally, if a shipboard compatibility requirement were imposed

Table 7. Gross weight growth factors for high-speed tilt-rotor designs

	Percent gross weight increase	
	Civil transport	Air-combat fighter
Added weight, 10% increase	15	19
Airframe drag, 10% increase	2	5
Rotor efficiency, 10% decrease	3	8
Wing stiffness, 10% increase	1	1.5
Wing thickness, 10% decrease	0.5	0.6
Ship-board compatibility	---	6

on the air-combat tilt rotor, involving rotor/wing-fold capability and a wing-fold fairing, a 6% weight penalty would be incurred for the design.

8.2. Comparisons with Other Aircraft

Comparison of the present designs with the XV-15 and V-22 illustrates the influence of speed on the basic design parameters. The high-speed designs have a lower rotor tip speed in cruise (Table 4). Both aircraft are designed to operate at a helical-tip Mach number of about 0.80; the lower tip speed of the civil transport reflects the lower speed of sound at an altitude of 20,000 ft. The dominance of the cruise-operating condition results in a larger disk loading for the high-speed designs; hence, a larger solidity, since the blade loading must be about the same. The importance of the airframe drag at high speed is reflected in the lower fuselage-drag coefficients.

The high-speed civil transport is about the same size as the V-22 (Table 4), although it has smaller rotors. The significantly smaller drag of the civil transport is reasonable since the V-22 is a lower-speed, military aircraft. Hence, the power-loading or cruise efficiency is better than that of the V-22.

A conventional turboprop aircraft, designed using current technology to carry 46 passengers, would have a gross weight of 36,000-41,000 lb. The high-speed tilt-rotor design is within that range--advanced technology offsets the impact of the vertical flight capability. There are a number of current turboprop aircraft of this size: the Fokker F27, the British Aerospace BAe748, and the de Havilland DHC-7. These aircraft have gross weights of around 46,000 lb, but their cruise speeds are under

300 knots. A wing loading of 50-60 lb/ft^2 is typical of a 40,000-lb turboprop aircraft. A tilt-rotor can use a higher wing loading, and hence achieve a better ride quality (90-100 lb/ft^2 would be typical of a small jet-transport aircraft or of a larger turboprop). An optimum tilt-rotor design has a different wing and rotor than the turboprop configuration: a turboprop typically has a wing-aspect ratio of 10 to 12, and rotor-disk loading of 140 to 220 lb/ft^2, and conventional turboprop has a power loading of 7.5 to 9 lb/hp. The power required for the high-speed tilt rotor is much greater. Yet with advanced technology, the tilt rotor can achieve almost the same cruise efficiency (current turboprops in the 40,000-lb weight class have $VW/P = 6.5$ to 7; for much larger turboprops, $VW/P = 8$ to 10 is typical). While the tilt rotor has more blade area and so operates at a lower C_T/σ than does a propeller, the penalty in propulsive efficiency is not great (Fig. 20), and with attention to the total drag, the penalty associated with low aspect ratio is minimized.

An advanced turboprop aircraft designed for the same speed and using the same level of advanced technology would be lighter than the tilt-rotor design presented here, and would have approximately 30% less installed power than the tilt rotor. However, the economic gains relative to current turboprops might not be enough to justify development of a new turboprop aircraft. In contrast, the tilt-rotor concept offers the option of using the advanced technology to pay for radically different capability, which should open up entirely new aircraft markets with new economic drivers.

The high-speed fighter design is smaller, yet heavier, than the XV-15 (Table 4). Its drag coefficient is higher than that of the civil transport, as expected for a military aircraft. However, the drag is still relatively low, implying a significant attention to airframe aerodynamics to achieve high speed. As a combat aircraft, the high-speed fighter design has a much higher power loading and lower cruise efficiency than the other tilt rotors.

Comparisons of the high-speed fighter design with other aircraft are not as straightforward as for the civil transport. Propeller-driven aircraft that can be considered are the Rockwell OV-10 (10,000-lb turboprop, but with a speed below 250 knots); and World War II fighters with speeds of almost 400 knots, especially the Lockheed P-38 (15,500-lb gross weight). Subsonic jet attack aircraft such as the Cessna A-37 (14,000 lb, and a speed of 440 knots) can also be considered. For these fixed-wing aircraft, a typical wing loading is 35 to 45 lb/ft^2, although it is larger for aircraft that are heavier or faster (e.g., the A-37 has a wing loading of 76 lb/ft^2). The aspect ratio of 5.5 for the OV-10 is the smallest of these aircraft. The OV-10 and P-38 have disk loadings of about 80 lb/ft^2, and have propellers about half the diameter as those of the tilt rotor. A power loading of 5.0 lb/hp

is typical; and the cruise efficiency is about 5 to 7, although the OV-10 has VW/P = 3.7.

The combat tilt-rotor design can also be compared with a high-speed helicopter. An advanced-technology, 200-knot helicopter would have a rotor solidity of about 0.10, a disk loading about 8 lb/ft^2; a blade loading about 80 lb/ft^2; a power loading of 4.5-6.2 lb/hp, and a cruise efficiency of VW/P = 2.8 to 3.8. The blade loading of the helicopter is determined by the lift limit of the edgewise-moving rotor in forward flight; hence, the blade loading is lower than that of a tilt rotor. At 225 knots, the helicopter design would have a solidity of about 0.15, a blade loading about 50 lb/ft^2, and a power loading of 2.8 to 4.2 lb/hp. The range of power values reflects the greater uncertainty in the design at 225 knots.

Such comparisons of the combat tilt rotor with other aircraft mainly serve to emphasize that it is a very different vehicle than those in current use, either airplane or helicopter. The tilt rotor has different capabilities, and hence it has very different design characteristics.

9. CONCLUSIONS

The designs presented in this paper illustrate the feasibility of a 400-knot tilting-prop-rotor aircraft. It has been possible to design highly efficient prop rotors and to handle the high speed stability requirement, with reasonable gross weights and installed power for the specified missions. As usual, the development of a new aircraft using medium-risk technology implies an extensive test program for early exposure and solution of problems.

While there are no apparent barriers to achieving major speed increases with the tilt-rotor concept, the present investigation has encountered several aspects of the technology that deserve additional research. In the aerodynamics design, the advanced airfoils considered represent existing technology. Further advances might be possible if the high-drag-divergence Mach numbers could be achieved with thicker airfoils. The predicted rotor performance using such airfoils needs experimental confirmation. Moreover, the aerodynamic optimization must be extended to cover multimission specifications.

In the dynamics design, the advanced hub considered here is at best representative of achievable technology. The predicted high-speed flap-lag and whirl-flutter stability characteristics need experimental confirmation. In particular, the minimum stability associated with the rotor-airfoil lift divergence must be verified. Little work has been done on the design of hubs and blades for tilt rotors; in contrast, substantial research is being

conducted on new concepts for helicopter rotors (e.g., as hingeless, bearingless, and soft, in-plane rotors). There should be great potential for hubs and blades optimized for tilt-rotor dynamics. Some work on detailed design of a representative aircraft would help further define the research needs, particularly in the dynamics field.

In the airframe aerodynamics, further analytical and wind tunnel tests will be required to assess the wing airfoil section design. The three-dimensional and interference transonic characteristics of the complete configuration must also be determined. Low airframe drag will be crucial to the success of a high-speed tilt rotor, particularly the avoidance of a large compressible drag rise before the design speed.

The representative high-speed designs presented in this paper were not intended to fit any design or consumer market. For the civil transport, the aircraft size was chosen so that the design would not be far from the existing tilt-rotor data base. A commercial 400-knot civil aircraft should probably have more cargo and/or passenger space and should have a longer range. The ideal civil VTOL aircraft must be able to hover with a minimal amount of aircraft noise, so as to not disturb the surrounding community. The tilt-rotor concept is inherently quiet in cruise and in tilt-rotor modes (with the rotors tilted enough that their wakes do not remain in the disk plane). For quiet hovering flight, the tiltrotor must be designed with low tip speeds in helicopter configuration. An investigation focused on the design of low noise in hover, would be appropriate. The present investigation does not indicate any additional technology issues that would be important for larger civil VTOL aircraft.

The air-combat fighter design presented here was based on the requirement for a 400-knot capability, to explore the technical implications of high speed. The actual mission requirement for a combat tilt rotor would probably be a somewhat lower speed, which would imply lower gross weight and power. Likely more emphasis would be placed on maneuver requirements and an increased payload. Also, fictitious engines were considered here, sized to meet the aircraft design requirements. A more realistic approach would be to develop the design around an existing or planned engine. Again, although there is much to consider in the preliminary design process, the present investigation does not indicate any additional technology issues as a consequence of such tradeoffs.

Having established that 400 knots is achievable, and defined the influence of high speed on the design characteristics, it is next possible to begin the task of balancing the value and cost of such speed capability for various sizes and specific mission

requirements. Such continuing design activity will further define the potential of the tilting-prop-rotor concept.

10. REFERENCES

1. Johnson, W. — A Comprehensive Analytical Model of Rotorcraft Aerodynamics and Dynamics. NASA TM 81182, 81183, and 81184 (1980)

2. Johnson, W. — Development of a Comprehensive Analysis for Rotorcraft. Vertica (1981) 5 (2-3)

3. Johnson, W. — Assessment of Aerodynamic and Dynamic Models in a Comprehensive Analysis for Rotorcraft. Comp. Math. with Applications (1986) 12A (1) 1986

4. Johnson, W. — Analytical Modeling Requirements for Tilting Proprotor Aircraft Dynamics. NASA TN D-8013 (1975)

5. Johnson, W. — An Assessment of the Capability to Calculate Tilting Prop-Rotor Aircraft Performance, Loads, and Stability. NASA TP 2291 (1984)

6. Bell Helicopter Company — Advancement of Proprotor Technology--Tunnel Test Results. NASA CR 114363 (1971)

7. Felker, F.F.; Maisel, M. D.; and Betzina, M. D. — Full Scale Tilt Rotor Hover Performance. J. Amer. Helicopter Soc. (1985)

8. Johnson, W. — Recent Developments in the Dynamics of Advanced Rotor Systems. AGARD Lec. Ser. No. 139 (1985); and NASA TM 86669 (1985)

9. Popelka, D.; Sheffler, M.; and Bilger, J. — Correlation of Stability Tests Results Analysis for the 1/5 Scale V-22 Aeroelastic Model. Annual Nat. Forum of Amer. Helicopter Soc. (1985)

10. Alexander, H.R.; Hengen, L. M.; and Weiberg, J. A.
Aeroelastic Stability Characteristics of a V/STOL Tilt-Rotor Aircraft with Hingeless Blades: Correlation of Analysis and Test.
J. Amer. Helicopter Soc. (1974) 20 (2)

11. Gaffey, T.M.
The Effect of Positive Pitch-Flap Coupling (Negative Delta-Three) on Rotor Blade Motion Stability and Flapping.
J. Amer. Helicopter Soc. (1969) 16 (2)

12. Hicks, R.M.
An Assessment of a Modified Potential Flow Code for Calculating the Effect of Small Geometric Change on the Pressure and Forces of Supercritical Airfoils.
NASA TM-84227 (1982)

13. McGhee, R.J., and Beasley, W. D.
Low-Speed Aerodynamic Characteristics of a 17-Percent Thick Medium-Speed Airfoil Designed for General Aviation Applications.
NASA TP 1786 (1980)

1. Report No.	2. Government Accession No.	3. Recipient's Catalog No.
NASA TM-88349		

4. Title and Subtitle	5. Report Date
CALCULATED PERFORMANCE, STABILITY AND MANEUVERABILITY OF HIGH-SPEED TILTING-PROP-ROTOR AIRCRAFT	September 1986
	6. Performing Organization Code
7. Author(s)	8. Performing Organization Report No.
Wayne Johnson, Benton H. Lau, and Jeffrey V. Bowles	A-86379
	10. Work Unit No.
9. Performing Organization Name and Address	11. Contract or Grant No.
Ames Research Center Moffett Field, CA 94035	
	13. Type of Report and Period Covered
12. Sponsoring Agency Name and Address	Technical Memorandum
National Aeronautics and Space Administration Washington, DC 20546	14. Sponsoring Agency Code 505-61-51

15. Supplementary Notes

Point of Contact: Benton Lau, Ames Research Center, M/S TA 32
Moffett Field, CA 94035 (415) 694-6653 or FTS 464-6653

16. Abstract

The feasibility of operating tilting-prop-rotor aircraft at high speeds is examined by calculating the performance, stability, and maneuverability of representative configurations. The rotor performance is examined in high-speed cruise and in hover. The whirl-flutter stability of the coupled-wing and rotor motion is calculated in the cruise mode. Maneuverability is examined in terms of the rotor-thrust limit during turns in helicopter configuration. The paper discusses rotor airfoils, rotor-hub configuration, wing airfoil, and airframe structural weights represent demonstrated advanced technology. Key rotor and airframe parameters are optimized for high-speed performance and stability. The basic aircraft-design parameters are optimized for minimum gross weight. To provide a focus for the calculations, two high-speed tilt-rotor aircraft are considered: a 46-passenger, civil transport and an air-combat/escort fighter, both with design speeds of about 400 knots. It is concluded that such high-speed tilt-rotor aircraft are quite practical.

17. Key Words (Suggested by Author(s))	18. Distribution Statement
Performance Stability Maneuverability Tilt-rotor aircraft	Unlimited Subject Category - 05

19. Security Classif. (of this report)	20. Security Classif. (of this page)	21. No. of Pages	22. Price*
Unclassified	Unclassified	45	A03

*For sale by the National Technical Information Service, Springfield, Virginia 22161